ARTICLE IN PRESS
JGLR-00846; No. of pages: 17; 4C: 7, 10, 12, 13, 14, 15
Journal of Great Lakes Research xxx (2015) xxx–xxx
Contents lists available at ScienceDirect
Journal of Great Lakes Research
journal homepage: www.elsevier.com/locate/jglr

# Modeling the effect of invasive quagga mussels on the spring phytoplankton bloom in Lake Michigan

M.D. Rowe [1,*], E.J. Anderson, J. Wang, H.A. Vanderploeg

*NOAA Great Lakes Environmental Research Laboratory, 4840 S State Rd., Ann Arbor, MI 48108, USA*

ARTICLE INFO

*Article history:*
Received 3 July 2014
Accepted 2 December 2014
Available online xxxx

Communicated by Hunter Carrick

*Index words:*
Numerical modeling
Lake Michigan
Phytoplankton
Quagga mussels

ABSTRACT

The disappearance of the spring phytoplankton bloom in Lake Michigan has been attributed in some studies to the direct effect of quagga mussel filter-feeding. We applied a biophysical model to test whether the observed reduction in the spring bloom can be explained by direct effects of quagga mussel grazing. We developed a 1-D column biological model that simulated light and temperature limitation on phytoplankton growth, vertical mixing, and grazing by zooplankton and quagga mussels. We applied the 3-D finite volume coastal ocean model (FVCOM) to provide vertical mixing, with two scenarios of atmospheric forcing: (a) North American Regional Reanalysis (NARR) and (b) station interpolation using the Natural Neighbor Method. Simulated development of the spring bloom and formation of the deep chlorophyll layer in the early summer stratified period were consistent with observations. Increased strength of winter stratification (surface < 4 °C) in 1997 (cold spring) increased chlorophyll concentrations during March and April, compared to 1998, by reducing light limitation (reduced mixed-layer depth). Simulations with NARR forcing produced high-biased chlorophyll, resulting from low-biased wind speed and spring mixed layer depth. Simulated mussel filter feeding strongly reduced phytoplankton abundance when the water column was mixed to the bottom, but had little effect during periods of summer and winter stratification. These model simulations highlight the sensitivity of both phytoplankton growth and the impact of profundal quagga mussel filter-feeding to vertical mixing and stratification, which in turn is controlled by meteorological conditions.

© 2015 International Association for Great Lakes Research. Published by Elsevier B.V. All rights reserved.

## Introduction

The population of non-indigenous quagga mussels (*Dreissena rostriformis bugensis*) expanded rapidly in Lake Michigan over the period 2000–2005 (Nalepa et al., 2009). Over the same period, the spring phytoplankton bloom was greatly reduced (Yousef et al., 2014). Earlier studies (Fahnenstiel et al., 2010; Vanderploeg et al., 2010) attributed the disappearance of the spring bloom to the direct effect of quagga mussel filter-feeding on phytoplankton, arguing that observed mussel abundance and clearance rates could outpace phytoplankton growth, under the assumption of a well-mixed water column during the spring isothermal period. Later studies observed reduced chlorophyll in the deep chlorophyll layer (DCL) during summer stratification, in addition to reduced spring chlorophyll, and discussed the influence of quagga mussels on phosphorus cycling and distribution (Pothoven and Fahnenstiel, 2013).

Stratification and vertical mixing have a strong influence on phytoplankton growth and on the coupling of benthic filter feeders to the euphotic zone. Lake Michigan is thermally stratified during the summer, approximately May through October, and vertically well-mixed when the surface temperature reaches 4 °C in fall and spring. The summer surface mixed layer (SML) depth may reach the bottom in nearshore areas with depth < ~20–30 m, resulting in intermittent periods of stratification and mixing in the nearshore. Ice cover and winter stratification (surface temperature < 4 °C) develop to some extent each year, but the spatial extent and duration are highly variable among years (Wang et al., 2012).

The spring phytoplankton bloom occurs under conditions of deep mixing in which light limitation plays an important role, as the SML depth is large relative to the euphotic zone depth for much of the lake (Fahnenstiel et al., 2000; Vanderploeg et al., 2007). The mean light exposure to phytoplankton cells depends on the euphotic zone depth as a fraction of the SML depth (Fahnenstiel et al., 2000). The SML is limited by bathymetric depth during the unstratified period, and by the balance between static stability and mechanical mixing during the stratified period. The direct effect of mussel filter feeding on phytoplankton is mainly limited to the unstratified period (Vanderploeg et al., 2010), when turbulent mixing effectively transports phytoplankton between the euphotic zone and the benthos.

During the stratified period, mussels may depend on lateral transport of food particles. It has been hypothesized that interception of cross-isobath transport of organic particles by dreissenid mussels

* Corresponding author.
*E-mail address:* mark.rowe@noaa.gov (M.D. Rowe).
[1] National Research Council Research Associate.

http://dx.doi.org/10.1016/j.jglr.2014.12.018
0380-1330/© 2015 International Association for Great Lakes Research. Published by Elsevier B.V. All rights reserved.

Please cite this article as: Rowe, M.D., et al., Modeling the effect of invasive quagga mussels on the spring phytoplankton bloom in Lake Michigan, J. Great Lakes Res. (2015), http://dx.doi.org/10.1016/j.jglr.2014.12.018

(*mid-depth sink*, (Vanderploeg et al., 2010)) has altered nutrient cycles. In 2008, the maximum biomass of quagga mussels occurred in the 30–50 m depth range (Nalepa et al., 2010); prior to the quagga mussel invasion, a pronounced benthic nepheloid layer (BNL) existed during the stratified period in the same depth range. The BNL was believed to be caused by oscillating currents at a near-inertial period associated with internal waves in the stratified water column, although the exact mechanism of particle resuspension was unclear (Hawley, 2004). In biophysical models, simulation of the near-inertial period oscillating currents is of interest in order to characterize the physical environment where quagga mussels currently reside, and which formerly supported the BNL.

Hydrodynamic modeling studies in Lake Michigan have often focused on general circulation patterns and thermal structure during the summer stratified period. For example, an application of Princeton Ocean Model (POM) on a 2-km grid simulated circulation patterns with greater skill than a 5-km grid model, but problems with shallow mixed layer depth and diffuse thermocline persisted (Beletsky et al., 2006). Bai et al. (2013) applied the Finite-Volume Coastal Ocean Model (FVCOM) to simulate climatological-mean circulation patterns and thermal structure in all five Great Lakes. Relatively few studies have focused on the unstratified period, and few studies have tested the sensitivity of vertical mixing to alternate sources of forcing conditions. In one example, a POM simulation of a March 1998 storm event revealed that forcing by the MM5 meteorological model, versus interpolated observed winds, resulted in improved simulation of currents (Beletsky et al., 2003). Both types of forcing resulted in overestimated vertical gradients in simulated currents (their Fig. 8), suggesting low-biased vertical mixing during the unstratified period.

Biophysical modeling studies in Lake Michigan have not focused on simulation of the vertical distribution of chlorophyll, nor on the impact of quagga mussel grazing on chlorophyll concentration. An application of FVCOM to Lake Michigan with coupled nutrient–phytoplankton–zooplankton–detritus model (NPZD), focused on simulation of the spatial distribution of surface chlorophyll prior to the quagga mussel invasion; they attributed formation of the 'doughnut' shaped spring phytoplankton bloom observed in satellite imagery primarily to physical processes, including constrained nearshore–offshore transport by the thermal bar (Luo et al., 2012). An application of POM with a coupled lower food web model focused on the impacts of sediment resuspension events on the lower food web in March during the pre-mussel period, but did not extend simulations into the summer stratified period (Chen et al., 2004). Pauer et al. (2008) applied a linked lower food web model forced by a 5-km grid POM simulation for 1994–95 to evaluate the impacts of phosphorus loading on chlorophyll and phosphorus concentration in the pre-mussel period. Most Great Lakes biophysical models have neglected photoacclimation of phytoplankton and applied a fixed chlorophyll to carbon ratio, although White et al. (2012) recently applied the photoacclimation model of Geider et al. (1997) in Lake Superior.

We applied a biophysical model to test whether the observed reduction in the spring phytoplankton bloom after ~2004 can be explained by direct, local effects of quagga mussel grazing. We developed a 1-D column phytoplankton model based on the Great Lakes Primary Production model, and extended the model to simulate phytoplankton growth rate, chlorophyll concentration, and variable chlorophyll to carbon ratio (photoacclimation). The biophysical model simulated light limitation, vertical mixing, and grazing by zooplankton and quagga mussels. We used photosynthesis-irradiance parameters that were measured in Lake Michigan at ambient nutrient concentrations, representative of nutrient-limited values during the 1980s, but we did not simulate spatial and temporal variation in nutrient limitation. Dreissenid mussels remove particulate phosphorus from the water column, and excrete soluble phosphorus along with particulate feces and pseudofeces; the net effect on phosphorus cycling may be either to enhance or retard phytoplankton growth (Bocaniov et al., 2014; Zhang et al., 2011). By not simulating dynamic nutrient limitation, we isolate the direct impact of mussel grazing on phytoplankton from feedback effects on phosphorus cycling. We applied the 3-D finite volume coastal ocean model (FVCOM) to provide realistic vertical mixing. We selected 1997 and 1998 to represent pre-mussel years that were colder than normal and warmer than normal, respectively (Vanderploeg et al., 2012) to show the effect of varying meteorological conditions on phytoplankton growth and mussel grazing impacts. A secondary objective of this study was to assess the model sensitivity to atmospheric forcing and evaluate the ability of the hydrodynamic model to simulate physical features that would be important not only for the 1-D biological model applied here, but also in future applications of more complex 3D biogeochemical models; these features included currents and vertical mixing during the unstratified season, spatial extent and duration of stratification, surface mixed layer depth, and near-inertial period oscillating currents during the stratified season.

## Methods

### *Hydrodynamic model*

FVCOM (v. 3.1.6) is an unstructured grid, finite-volume, free surface, three-dimensional primitive equation ocean model that solves the momentum, continuity, temperature, salinity, and density equations (Chen et al., 2003). Turbulence closure is implemented through the MY-2.5 scheme for vertical mixing (Galperin et al., 1988) and the Smagorinsky scheme for horizontal mixing. We applied the model to Lake Michigan with 20 sigma layers of uniform thickness. The unstructured grid consisted of 5795 nodes and 10,678 elements, with element side lengths of 0.6 to 2.6 km near the coast and 4.5 to 6.8 km near the center of the lake (median 3.1 km). The lateral boundaries were closed, including the Straits of Mackinac (Fig. 1). Bathymetry was interpolated from the NOAA National Geophysical Data Center (www.ngdc.noaa.gov/mgg/greatlakes/greatlakes.html). The model was initialized on January 1, 1997 or 1998, with uniform temperature of 4 °C (obtained from NOAA CoastWatch Great Lakes Surface Environmental Analysis (GLSEA), see Observational data), and salinity and current velocities set to zero. Surface fluxes of momentum, sensible heat, and latent heat were calculated by the NOAA COARE bulk algorithm (v. 2.6) (Fairall et al., 1996). External and internal time steps were 10 s. The coefficient used in the Smagorinsky scheme for horizontal mixing was set to 0.1, and the minimum bathymetric depth was 0.1 m. Light penetration length scales were set to 5.0 m (equivalent to a diffuse attenuation coefficient of 0.2 $m^{-1}$), based on analysis of light penetration profiles collected in Lake Michigan during the 1990s.

### *Atmospheric forcing*

We evaluated two sources of atmospheric forcing data in order to determine which one would provide the most accurate simulations of temperature fields, currents, and stratification for use in the biological model: one scenario with atmospheric forcing interpolated from land-based and buoy meteorological stations using the Natural Neighbor Method (NNM) (referred to here as "Interpolated forcing" or "interp") and the other with atmospheric forcing from the North American Regional Reanalysis (NARR). Atmospheric forcing variables were *U* and *V* components of 10-m wind velocity, air temperature, relative humidity, downward shortwave, and downward longwave radiation. Upward longwave radiation was calculated in FVCOM using the simulated water surface temperature.

The interpolated forcing scenario was generated using computer codes developed for use in the NOAA Great Lakes Coastal Forecasting System, which were described in detail elsewhere (Beletsky et al., 2003; Schwab and Beletsky, 1998). Hourly atmospheric forcing variables of wind speed, wind direction, air temperature, dewpoint temperature, and cloud cover were interpolated over Lake Michigan from 18 land-based meteorological stations. In addition, wind speed, direction,

ARTICLE IN PRESS



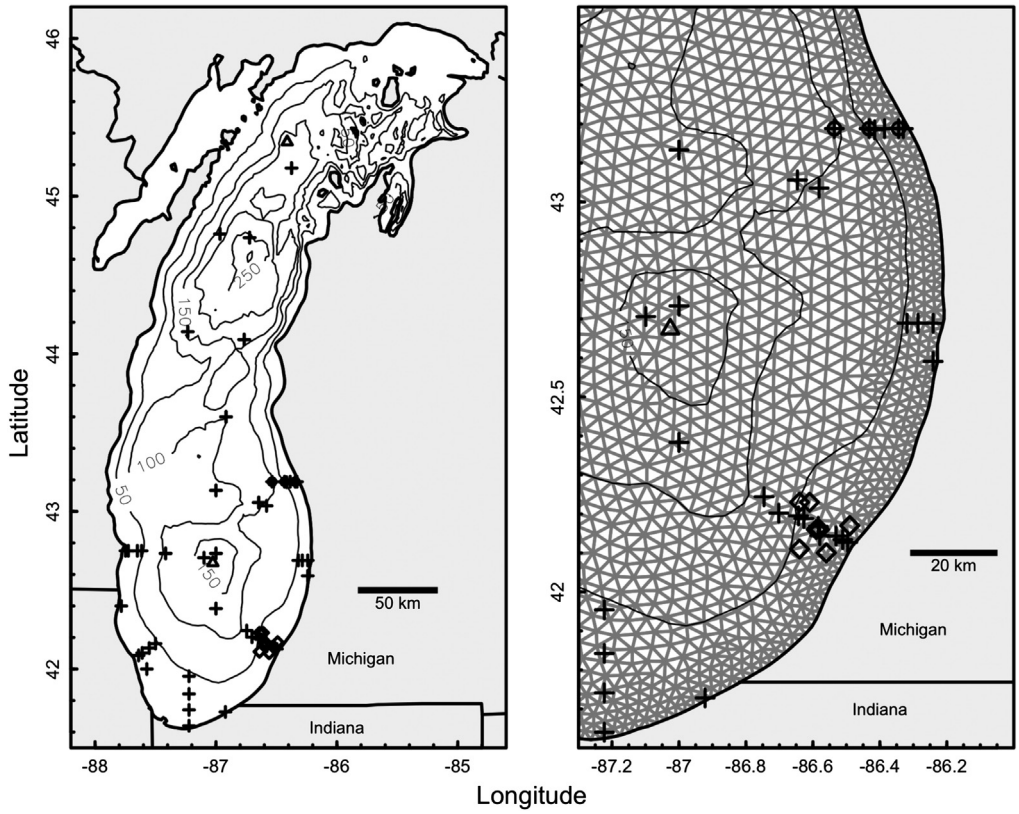


**Fig. 1.** Map of Lake Michigan. Left panel: Spatial domain of the hydrodynamic model (white area), bathymetry (50-m contours), and locations of NOAA buoys (triangles), temperature profile stations (crosses), ADCP stations (diamonds), and stations M110, M45, and M15 (circles). Right panel: Enlarged area of southeastern Lake Michigan, showing a portion of the unstructured hydrodynamic model grid and station locations.

and air temperature were used in the interpolation from NOAA buoys 45002 and 45007, located in northern and southern Lake Michigan, respectively (Fig. 1). Wind speeds were adjusted to 10-m height. Empirical relationships were used to adjust land-based meteorological variables for over-lake modification,

$$U_w = U_L\left(1.2 + \frac{1.85}{U_L}\right)\left[1 - \frac{\Delta T}{|\Delta T|}\left(\frac{|\Delta T|}{1920}\right)^{1/3}\right] \quad (1)$$

$$T_{aw} = AT_{al} + BT_w \quad (2)$$

$$T_{dw} = C + DT_{dl} + ET_w \quad (3)$$

where $U_w$, $T_{aw}$, and $T_{dw}$ are the overlake wind speed, air temperature, and dewpoint temperature, $A$, $B$, $C$, $D$, and $E$ are empirical constants, $U_L$, $T_{al}$, and $T_{dl}$ are the overland values, $T_w$ is the water surface temperature, and $\Delta T = T_{al} - T_w$, °C. Eq. (1) is from Resio and Vincent (see, Schwab and Morton, 1984). Eqs. (2)–(3) and empirical constants were derived from field experiments in Lake Ontario (Croley, 1989; Phillips and Irbe, 1978). Water surface temperature, for use in Eqs. (1)–(3), was the lakewide mean temperature from satellite remote sensing (see Observational data). Downward shortwave radiation and albedo were calculated with a global radiation, atmospheric transmission model, and downward longwave radiation was estimated as a function of air temperature and cloud cover (Parkinson and Washington, 1979).

The second set of atmospheric forcing data was obtained from North American Regional Reanalysis (NARR). NARR is 32-km-resolution data set derived from the NCEP Eta meteorological model with assimilation of observational data from surface, upper atmosphere, and remote sensing sources, including Great Lakes buoy data and satellite-derived surface temperature (Mesinger et al., 2006, www.esrl.noaa.gov/psd/data/narr/, accessed May 2013). We interpolated 10-m $U$ and $V$ wind components, 2-m relative humidity, total cloud cover, net shortwave radiation, and downward longwave radiation to the model grid at a 3-hourly intervals.

*Biophysical model*

The scalar transport equation for the 1-D column phytoplankton model with sigma-stretched coordinate system was,

$$\frac{\partial B}{\partial t}D = \frac{1}{D}\frac{\partial}{\partial \sigma}\left(K_h\frac{\partial B}{\partial \sigma}\right) + DS \quad (4)$$

where $B$ is the phytoplankton biomass, $D$ is the total depth, $K_h$ is the vertical turbulent diffusivity for heat (assumed to apply to all scalar variables), and $S$ is the sink/source term calculated from the phytoplankton model. In this 1-D application, horizontal homogeneity was assumed, and water column depth was held constant for the duration of the simulation at the depth of the station being simulated (i.e., 15, 45, or 110 m). The transport equation was solved using an implicit scheme implemented in the vertical-mixing subroutine of the FVCOM-UBM model (Kim and Khangaonkar, 2012) and Euler-forward time integration with a 1-hour time step. Vertical diffusivity and water temperature were obtained from the 3-D hydrodynamic simulations at a specified node in the model domain. The sink/source term for phytoplankton biomass was,

$$S = \mu B_k + W_s(B_{k-1} - B_k) - g_z - g_m \quad (5)$$

where $\mu = P^C - R$ is the growth rate, $P^C$ is the carbon-specific photosynthetic rate, $R$ is the respiration rate, $W_s$ is the settling velocity, $k$ is the index of the sigma layer, $g_z$ is the loss due to grazing by zooplankton,

Please cite this article as: Rowe, M.D., et al., Modeling the effect of invasive quagga mussels on the spring phytoplankton bloom in Lake Michigan, J. Great Lakes Res. (2015), http://dx.doi.org/10.1016/j.jglr.2014.12.018

ARTICLE IN PRESS



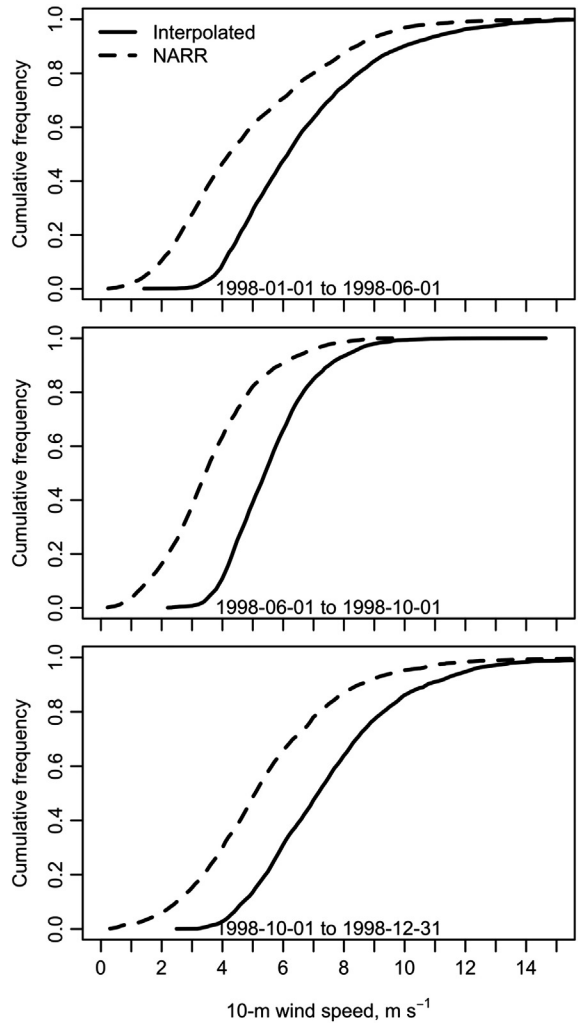


**Fig. 2.** Cumulative frequency distribution of wind speed from interpolated forcing and NARR forcing at the location of the ADCP stations in southeastern Lake Michigan (Fig. 1) for winter/spring (top panel), summer (middle panel), and fall (bottom panel) time periods.

and $g_m$ is the loss due to grazing by mussels (applied only at the bottom layer).

The positive contribution to phytoplankton biomass was provided by the Great Lakes Primary Production Model (Fahnenstiel et al., 1989; Lang and Fahnenstiel, 1996), which was used to calculate $P^C$,

$$P_s^{Chl} = P_m^{Chl}\frac{(\alpha+\beta)}{\alpha}\left(\frac{\beta}{\alpha+\beta}\right)^{\frac{-\beta}{\alpha}} \tag{6}$$

$$P^C = P_S^{Chl}\theta\left[1-exp\left(\frac{-\alpha I_{avg}}{P_S^{Chl}}\right)\right]exp\left(\frac{-\beta I_{avg}}{P_S^{Chl}}\right) \tag{7}$$

Where $P_m^{Chl}$ is the light-saturated, chlorophyll-specific photosynthetic rate, $P_m^{Chl}$ is a scaling parameter for the production–irradiance (PI) curve, $\alpha$ is the initial slope of the PI curve, $\beta$ is the negative slope of the PI curve at high irradiance (photoinhibition), $I_{avg}$ is the instantaneous irradiance averaged vertically over the model sigma layer. We modified the Great Lakes Primary Production Model to include $\theta$, the chl:C ratio, in order to output primary production normalized to carbon, rather than to chlorophyll. We used temperature-dependent $P_m^{Chl}$ and constant $\alpha$ values, reported by Fahnenstiel et al. (1989) for Lake Michigan (see Electronic Supplementary Material (ESM) for details of the model); these values represent nutrient limited conditions in Lake Michigan. Spatiotemporal variation in nutrient limitation was neglected in this study. We assume that the distribution of chlorophyll during the spring isothermal and early stratified periods is primarily a function of light limitation, temperature limitation, and vertical mixing; the validity of this assumption is tested by comparison of simulated to observed chlorophyll distribution (see Results and discussion). Fahnenstiel et al. (1989) found non-zero values of $\beta$ in some cases for the spring isothermal period, but our model was insensitive to $\beta$ over the observed range, so we used $\beta = 0$.

Irradiance was calculated in the water column as,

$$I_z = I_0 exp(K_{PAR}z) \tag{8}$$

where $I_0$ is the surface irradiance, $K_{par}$ is the attenuation coefficient for photosynthetically-active radiation (PAR), and $I_z$ is the irradiance at depth $z$ (negative) in the water column. We converted shortwave irradiance from the hydrodynamic forcing data to PAR using the approximations that 46% of shortwave irradiance is in the PAR waveband (400–700 nm), and 1 W m$^{-2}$ PAR $\approx$ 4.6 μmol quanta m$^{-2}$ s$^{-1}$ (Bleiker and Schanz, 1997). To obtain $K_{par}$, we fitted Eq. (8) to vertical profiles of PAR from the 1994–95 Lake Michigan Mass Balance study. We used $K_{par} = 0.27, 0.25, 0.22$ m$^{-1}$ for station depth ranges of 0–30, 30–60, and >60 m, respectively, based on median values for n = 50, 88, and 80 profiles, respectively. Light penetration in 1994–95 was representative of our simulation period of 1997–98, but light penetration increased in 2004 after the quagga mussel invasion (Barbiero et al., 2012). Our approach was to calibrate the model by comparison to observations from 1998, then show the simulated impact of quagga mussel grazing while holding all other variables constant, so we used the same $K_{par}$ values in the idealized quagga mussel grazing simulations.

Our model required a chlorophyll to carbon ratio, $\theta$, because our objective was to simulate chlorophyll concentration in addition to phytoplankton carbon, in contrast to the Great Lakes Primary Production Model, which used observed chlorophyll as an input and gives primary production as an output. Phytoplankton increase the chlorophyll content of their cells in low light, and decrease chlorophyll in high light, through the process of photoacclimation (Geider et al., 1997). Fahnenstiel and Scavia (1987) reported values of $\theta$ for Lake Michigan spring isothermal period, deep chlorophyll layer, and summer epilimnion that ranged from 0.09 to 0.02, and reported that shade adaptation was a significant factor in formation of the deep chlorophyll layer, along with in-situ growth, zooplankton grazing, and settling. Geider et al. (1997) developed a model of $\theta$ for conditions of balanced growth, under which phytoplankton cells regulate their pigmentation to balance the energy supplied by photosynthesis with the energy demand for growth. Geider et al. (1997) gave $\theta$ as,

$$\theta = \frac{\theta_m}{1+\left(\frac{\theta_m \alpha I_g}{2P_m^C}\right)} = \frac{\theta_m}{1+\left(\frac{I_g}{2K_I}\right)} \tag{9}$$

where $\theta_m$ is the maximum value of $\theta$ at low light, $P_m^C$ is the carbon-specific light-saturated gross photosynthetic rate, and $I_g$ is the irradiance averaged over the time scale of photoacclimation, which we took to be ~24 h (Geider et al., 1998, their Fig. 9). The parameter $K_I = P_m^C/\alpha\theta_m$ represents the irradiance at which growth is light-saturated and represents a lower limit on $I_k = P_m^{chl}/\alpha$, the light saturation parameter for photosynthesis (Geider et al, 1997). To apply Eq. (9) in our model, $P_m^C$ was calculated as $P_m^C = P_m^{chl}\theta_{t-1}$, where $\theta_{t-1}$ was the value of $\theta$ from the previous time step; $\theta$ converged on the updated value with a few time steps after $I_g$ was updated. Phytoplankton living within a turbulent mixed layer are exposed, on average, to the mean irradiance over the mixed layer. Therefore, we estimated $I_g$ by averaging irradiance within each sigma layer over 24 h, and vertically over the SML. We defined the SML as all layers from the surface downward to the first layer having a value of $K_h < 10^{-3}$ m$^2$ s$^{-1}$, which corresponds to a mixing time

Please cite this article as: Rowe, M.D., et al., Modeling the effect of invasive quagga mussels on the spring phytoplankton bloom in Lake Michigan, J. Great Lakes Res. (2015), http://dx.doi.org/10.1016/j.jglr.2014.12.018

ARTICLE IN PRESS



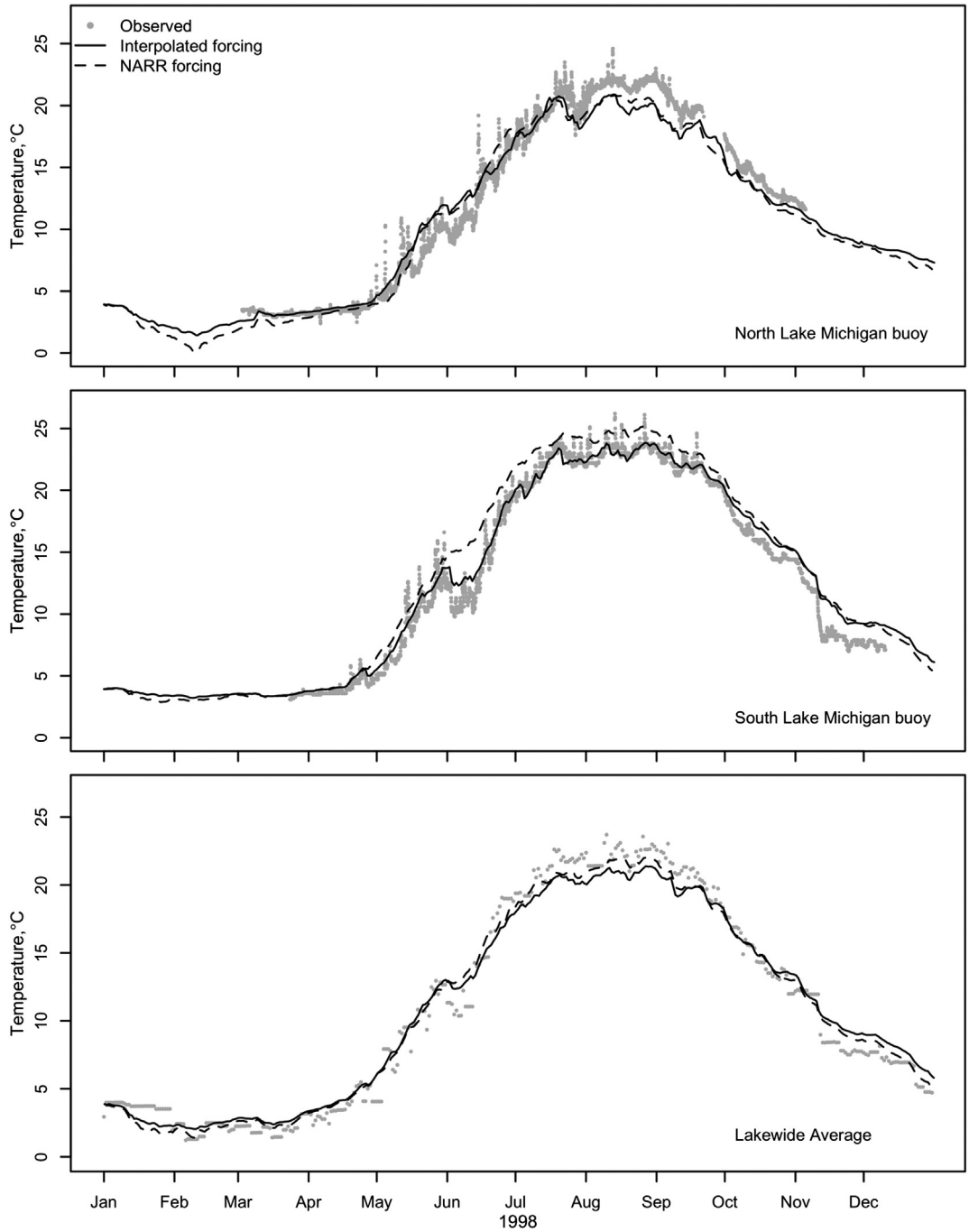


**Fig. 3.** Comparison of simulated to observed surface temperatures for two atmospheric forcing scenarios at the north and south Lake Michigan buoys (Fig. 1) and for the satellite-derived GLSEA lakewide mean surface temperature.

scale of ~24 h for a 10-m surface mixed layer. We set $\theta_m$ to 0.060 and limited $\theta$ to a minimum value of 0.026 through analysis of $\theta$ values for Lake Michigan reported by Fahnenstiel and Scavia (1987; see ESM for additional details).

**Table 1**
Surface temperature model skill statistics, °C, for 1998: bias deviation (BD) and root-mean-square deviation (RMSD).

| | North buoy | | South buoy | | Lakewide mean | |
|---|---|---|---|---|---|---|
| Forcing | BD | RMSD | BD | RMSD | BD | RMSD |
| Interpolated | −0.3 | 1.3 | 0.6 | 1.1 | 0.0 | 1.1 |
| NARR | −0.4 | 1.2 | 1.5 | 1.9 | 0.0 | 1.0 |

Negative contributions to phytoplankton biomass included respiration, grazing, and settling. Respiration was calculated as,

$$R = \zeta P^C - R_b \tag{10}$$

where $\zeta$ is the cost of biosynthesis, and $R_b$ is the dark respiration rate. In this model, $R$ may be considered to represent the sum of respiration and excretion of dissolved organic carbon (DOC); we do not simulate DOC concentration in the present application, so it is not necessary to treat respiration and excretion separately. We calibrated $\zeta$ to 0.3 and $R_b$ to 0.03 $d^{-1}$, within the range of reported values (Geider and Osborne, 1989), to achieve growth rates within the range of reported values (Scavia et al., 1988; see ESM for additional details).

Please cite this article as: Rowe, M.D., et al., Modeling the effect of invasive quagga mussels on the spring phytoplankton bloom in Lake Michigan, J. Great Lakes Res. (2015), http://dx.doi.org/10.1016/j.jglr.2014.12.018

ARTICLE IN PRESS



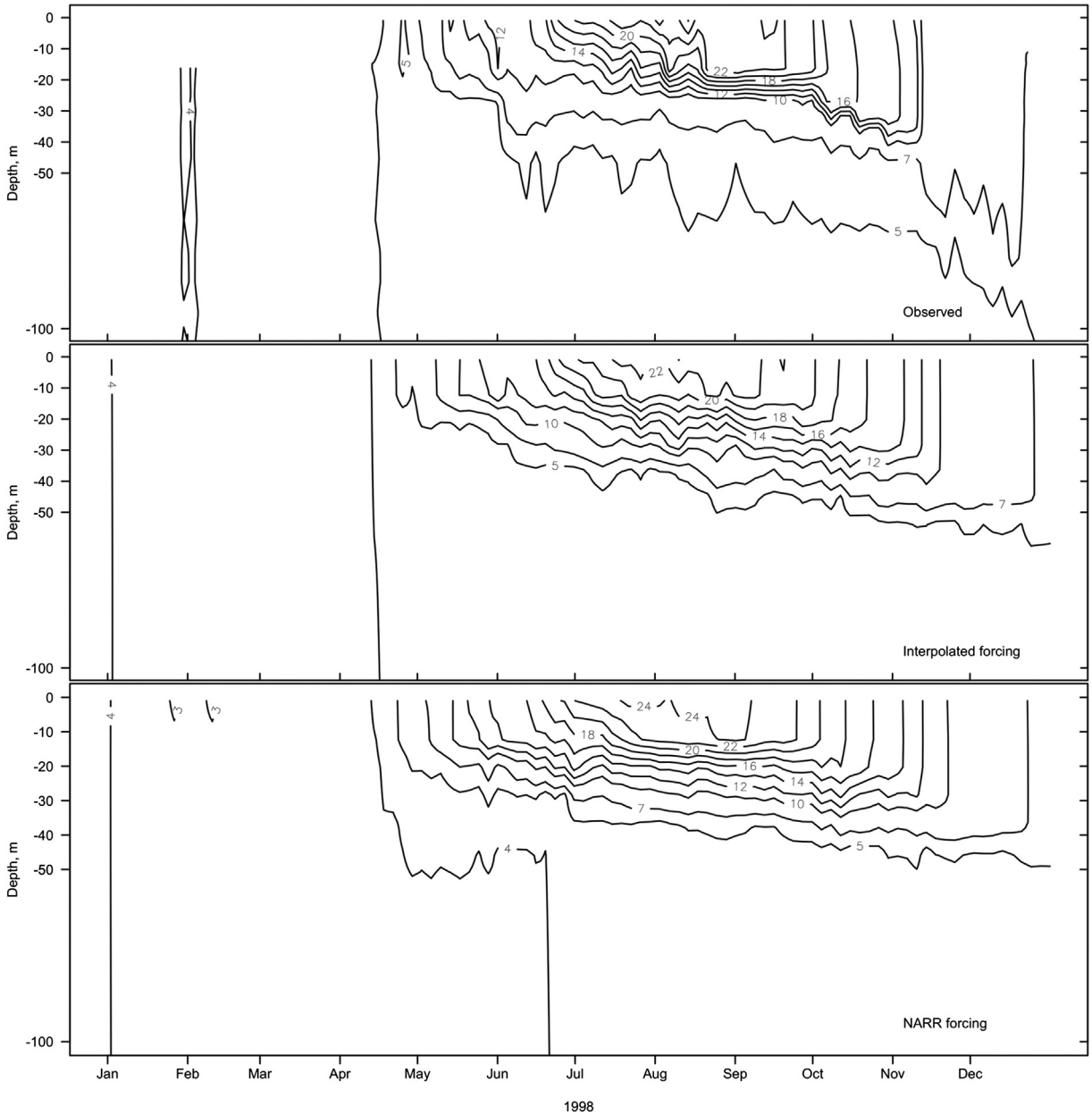


**Fig. 4.** Contour plots of observed and simulated thermal stratification at the southern Lake Michigan buoy (Fig. 1).

Grazing by zooplankton was simulated using a closure formulation, which assumes that predator biomass is directly proportional to prey biomass (e.g., Cerco and Noel, 2004; Fulton et al., 2003),

$$g_Z = K_{mpr} K_{pz} B \cdot f(B) \cdot f(T) \tag{11}$$

where $K_{mpr}$ is the zooplankton maximum specific ingestion rate, $K_{pz}$ is the ratio of zooplankton biomass to phytoplankton biomass, $f(B)$ and $f(T)$ are functions describing the influence of prey concentration and temperature, respectively, on the specific ingestion rate (see ESM). We set $K_{pz}$ to a rough estimate of 1 (Fahnenstiel et al., 1998, their Fig. 11; Scavia et al., 1988, their Table 4) and calibrated $K_{mpr}$ to a value of 0.6 $d^{-1}$ (e.g., ~0.2 to 0.86 $d^{-1}$, Scavia et al., 1988) to achieve a maximum chlorophyll concentration during early stratification within the range of observed values prior to addition of grazing by mussels.

Grazing of phytoplankton by mussels was calculated as,

$$g_M = \frac{B_M B F_A}{D\sigma} \tag{12}$$

where $B_M$ is the dreissenid mussel biomass per unit area, and $F_A$ is the mussel clearance rate. Grazing by mussels was applied only to the bottom layer of the model. Dreissenid biomass reached 20 g ash-free-dry-weight (AFDW) per square meter in 2005 in the 30–50 m depth range in southern Lake Michigan, while it was < 5 g $m^{-2}$ in < 30, 50–90, and >90-m depth ranges (Nalepa et al., 2010). In order to focus

**Table 2**
Model skill statistics for 1998 at the CTD profile stations (Fig. 1) for number of simulated:observed stratified profiles (No. strat.), surface mixed layer depth (SML depth, m), and thermocline gradient (Gradient, °C/m).

| | | SML depth | | Gradient | |
|---|---|---|---|---|---|
| Forcing | No. strat. | BD | RMSD | BD | RMSD |
| Interpolated | 30:32 | 5.2 | 6.9 | −1.0 | 1.3 |
| NARR | 47:32 | 6.6 | 8.4 | −0.8 | 1.1 |

Please cite this article as: Rowe, M.D., et al., Modeling the effect of invasive quagga mussels on the spring phytoplankton bloom in Lake Michigan, J. Great Lakes Res. (2015), http://dx.doi.org/10.1016/j.jglr.2014.12.018

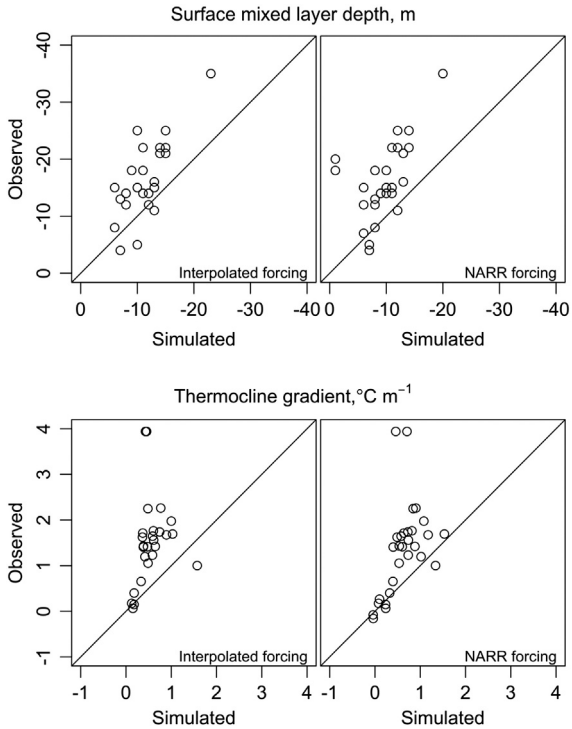


**Fig. 5.** Scatter plots of observed (stratified CTD profiles n = 32) versus simulated surface mixed layer depth (as negative meters) and thermocline gradient for the two atmospheric forcing scenarios.

our analysis on the sensitivity of mussel grazing impacts to bathymetric depth and vertical mixing, we applied a constant mussel biomass of 20 g AFDW m$^{-2}$ in each model scenario. We obtained temperature-

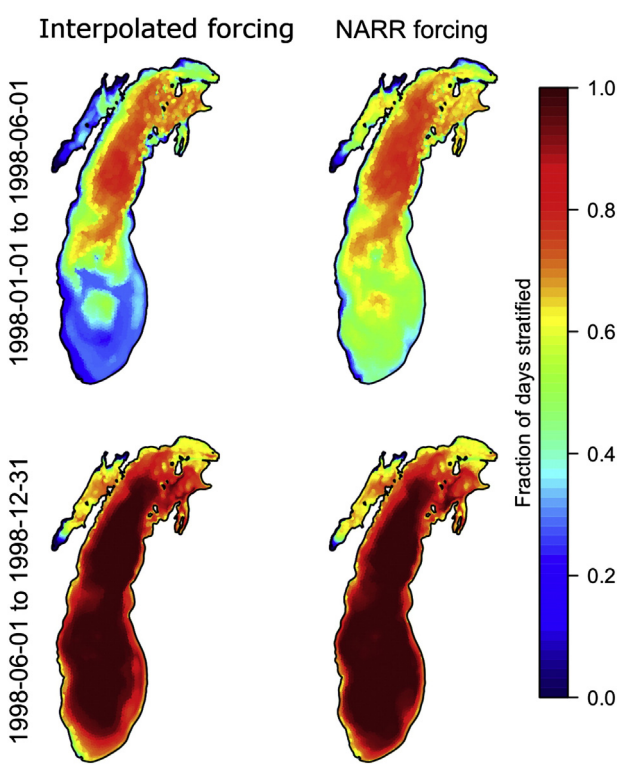


**Fig. 6.** Spatial extent and duration of simulated stratification for winter and summer periods and two atmospheric forcing scenarios. Occurrence of stratification was defined as a value of potential energy anomaly > 0.4 J m$^{-3}$.

**Table 3**
Model skill statistics for currents at the ADCP stations (Fig. 1), bias deviation (BD), root mean square deviation (RMSD), Fourier norm ($F_n$), and the average angle difference $\langle\theta\rangle$ for current speed and velocity during the unstratified period (Jan 1 to April 15, 1998) and stratified period (June 1 to October 1, 1998).

| | | | Current speed, cm s$^{-1}$ | | | Velocity | |
|---|---|---|---|---|---|---|---|
| Forcing | Period | Layer | BD | RMSD | Obs. mean | $F_n$ | $\langle\theta\rangle$ |
| Interpolated | Unstratified | All | −0.8 | 5.4 | 8.2 | 0.64 | 0.24 |
| NARR | Unstratified | All | −3.5 | 6.8 | 8.2 | 0.72 | 0.26 |
| Interpolated | Stratified | Surface | −4.1 | 11.5 | 16.1 | 0.83 | 0.29 |
| NARR | Stratified | Surface | −5.6 | 11.8 | 16.1 | 0.85 | 0.33 |
| Interpolated | Stratified | Bottom | −3.7 | 7.5 | 12.1 | 0.91 | 0.31 |
| NARR | Stratified | Bottom | −6.5 | 9.2 | 12.1 | 0.99 | 0.36 |

dependent $F_A$ from the linear regression of Vanderploeg et al. (2010, their Fig. 2). We used the values based on their experiments feeding quagga mussels on *Cryptomonas* to simulate a high feeding rate on a favorable food source, and limited $F_A$ at temperatures > 7 °C to 25 mL mg AFDW$^{-1}$ h$^{-1}$; observed values of $F_A$ for Lake Michigan quagga mussels showed no significant temperature dependence over the range 7–25 °C (Vanderploeg et al., unpublished data). For the purpose of comparison to clearance rates reported on an individual basis, a clearance rate of 25 mL mg AFDW$^{-1}$ h$^{-1}$ would be equivalent to 383 mL individual$^{-1}$ h$^{-1}$ for a Lake Michigan profunda-morph quagga mussel of 21.5 mm length and 15.3 mg AFDW (Vanderploeg et al., 2010, mean length and weight from their Table 3).

*Characterization of the physical environment for phytoplankton growth*

The physical environment for phytoplankton growth in a turbulent mixed layer can be characterized by two parameters: the

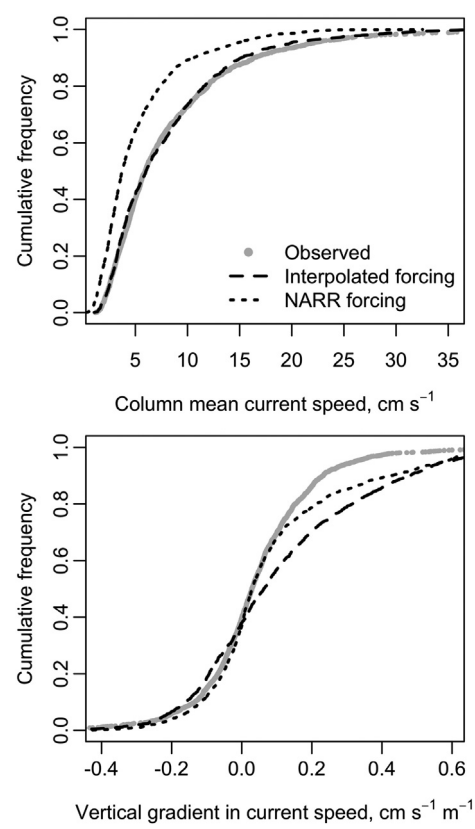


**Fig. 7.** Simulated and observed cumulative frequency distribution of column-mean current speed and vertical gradient in current speed at the ADCP stations (Fig. 1) for the unstratified period (Jan 1 to April 15, 1998).

Please cite this article as: Rowe, M.D., et al., Modeling the effect of invasive quagga mussels on the spring phytoplankton bloom in Lake Michigan, J. Great Lakes Res. (2015), http://dx.doi.org/10.1016/j.jglr.2014.12.018

ARTICLE IN PRESS



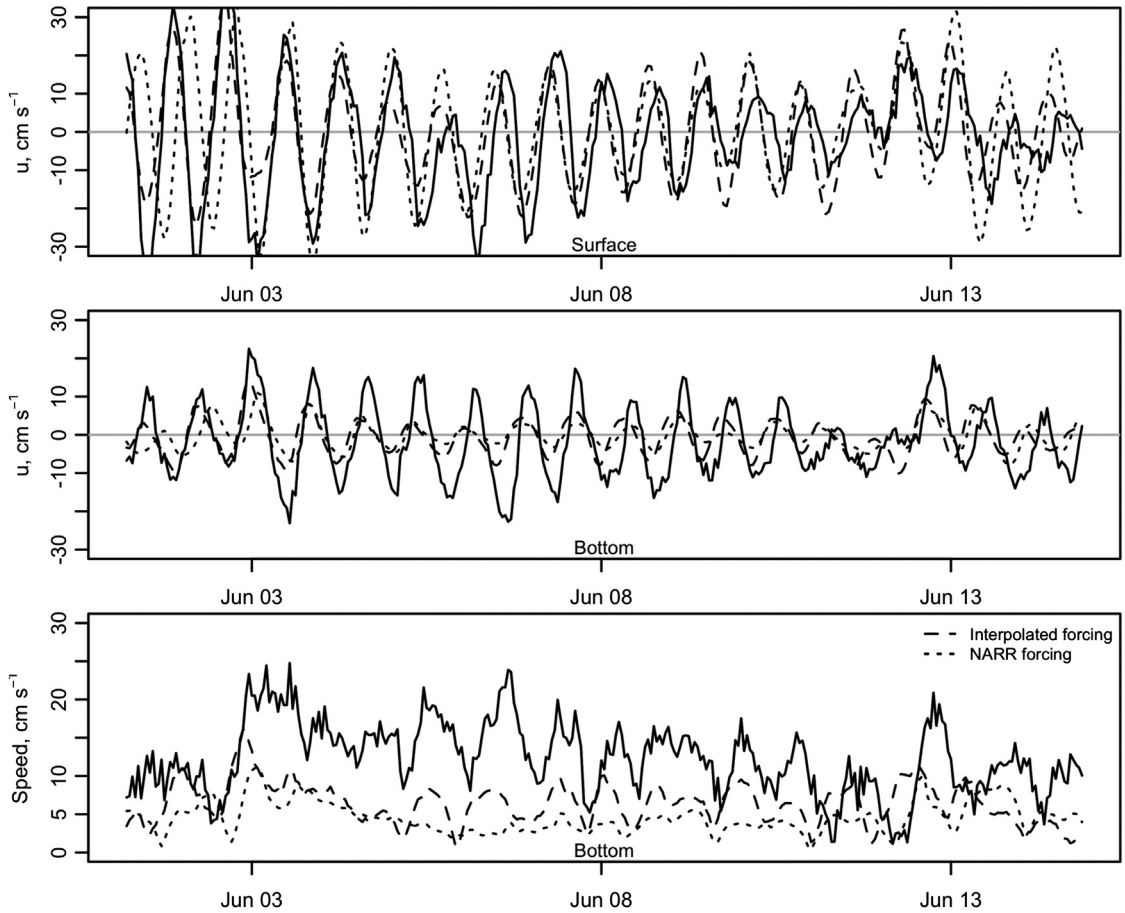


**Fig. 8.** Time series of simulated and observed eastward current velocity ($u$) at the surface (top panel); current velocity ($u$) and current speed at the bottom (middle and bottom panels) at a 38-m depth ADCP station (Fig. 1) in June 1998. Solid line is observed data.

vertical mixing time scale, and the light attenuation relative to the SML depth (Ross et al., 2011). The vertical mixing time scale is given by,

$$\tau_m = \frac{{z_m}^2}{K_h} \tag{13}$$

where $z_m$ is the SML depth. Fahnenstiel et al. (2000) quantified light attenuation relative to SML depth as,

$$\%\bar{I}_{zm} = \frac{z_E}{4.6 z_m}\left[1 - exp\left(-4.6\frac{z_m}{z_E}\right)\right] \cdot 100\% \tag{14}$$

where $z_E = -4.6/K_{par}$ is the euphotic zone depth, defined at 1% of surface irradiance, and $\%\,\bar{I}_{zm}$ represents mean irradiance in the SML as a percentage of surface irradiance. Finally, the SML depth is strongly influenced by the static stability of the water column, which can be quantified using the potential energy anomaly, φ,

$$\varphi = \frac{1}{D}\int_0^D (\hat{\rho} - \rho) g z dz; \;\; \hat{\rho} = \frac{1}{D}\int_0^D \rho dz \tag{15}$$

where $\rho$ is the local density, and $g$ is acceleration due to gravity (Simpson and Bowers, 1981; Wiles et al., 2006).

*Observational data*

Observational physical data included surface, subsurface, and remote sensing temperature measurements, in addition to currents measured by acoustic Doppler current profilers (ADCP). Water surface temperature was obtained from NOAA buoys 45002 and 45007 in north and south Lake Michigan, respectively (www.ndbc.noaa.gov/, accessed January 2013). Satellite-derived water surface temperature was obtained from NOAA CoastWatch Great Lakes Surface Environmental Analysis (GLSEA) (http://coastwatch.glerl.noaa.gov/glsea/glsea.html, accessed January 2013). The NOAA Episodic Events — Great Lakes Experiment (EEGLE) study provided ship-based vertical temperature profiles (CTD), ADCP, and thermistor measurements (http://www.glerl.noaa.gov/eegle/data/, accessed January 2013). ADCPs were deployed at four moorings at 18 and 38 m depth in southeastern Lake Michigan. Additional temperature and PAR profile data were obtained from US EPA spring and summer surveys (www.epa.gov/greatlakes/monitoring/data_proj, accessed April 2012). Chlorophyll-a concentration and column-integrated primary production were measured at long-term ecological research stations located offshore from Muskegon at 110, 45, and 15 m bathymetric depths, M110, M45, and M15, respectively, detailed methods are reported by Fahnenstiel et al. (2010). Station locations are indicated in Fig. 1.

Hydrodynamic model skill for scalar quantities was assessed using the bias deviation (BD) and root mean square deviation (RMSD),

$$BD = \frac{1}{n}\sum_{i=1}^{n}(s_i - o_i) \tag{16}$$

$$RMSD = \left[\frac{1}{n}\sum_{i=1}^{n}(s_i - o_i)^2\right]^{1/2} \tag{17}$$

where $s_i$, $o_i$ are the simulated and observed values at a given location

Please cite this article as: Rowe, M.D., et al., Modeling the effect of invasive quagga mussels on the spring phytoplankton bloom in Lake Michigan, J. Great Lakes Res. (2015), http://dx.doi.org/10.1016/j.jglr.2014.12.018

ARTICLE IN PRESS



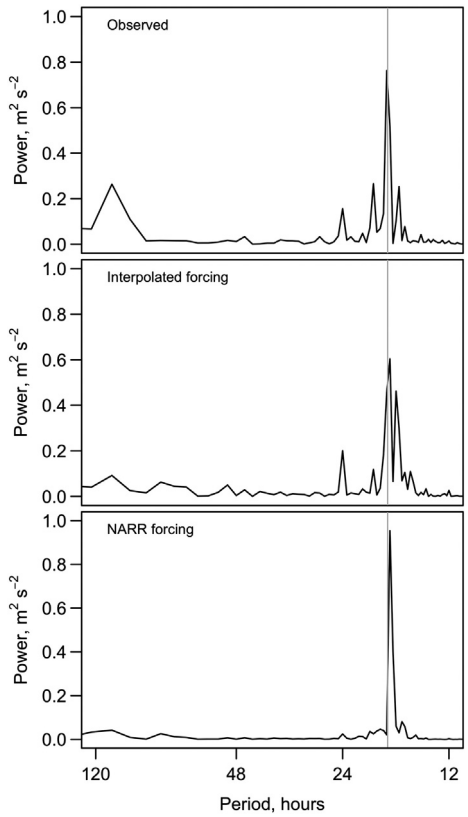


**Fig. 9.** Periodograms of observed and simulated eastward surface current velocity for a 35-day period beginning 1998-08-26 at a 38-m deep ADCP station (Fig. 1). The vertical gray line indicates the inertial period of 18 h.

and time, and $n$ is the number of observations. To assess model skill for current vectors, we used the normalized Fourier norm ($F_n$) and the average angle difference $\langle\theta\rangle$ (Schwab, 1983),

$$F_n = \frac{\|\mathbf{v}_o, \mathbf{v}_s\|}{\|\mathbf{v}_s, 0\|} = \frac{\left(\frac{1}{n}\sum_{i=1}^{n}|\mathbf{v}_{oi}-\mathbf{v}_{si}|^2\right)^{1/2}}{\left(\frac{1}{n}\sum_{i=1}^{n}|\mathbf{v}_{oi}-0|^2\right)^{1/2}} \tag{18}$$

$$\langle\theta\rangle = \frac{1}{\pi n}\sum_{i=1}^{n} cos^{-1}\left(\frac{\mathbf{v}_{oi}\cdot\mathbf{v}_{si}}{|\mathbf{v}_{oi}||\mathbf{v}_{si}|}\right) \tag{19}$$

where $\mathbf{v}_s$, $\mathbf{v}_o$ are the simulated and observed current vectors at a given place and time. For perfect agreement between simulated and observed currents, $F_n = 0$, values between 0 and 1 indicate improvement over the no-prediction case (zero simulated current), and greater than 1 indicates no improvement. A value of $\langle\theta\rangle = 0$ implies perfect directional agreement.

## Results and discussion

### *Hydrodynamic model skill assessment*

Hydrodynamic model skill assessment focused on 1998 because observational data were available from the EEGLE study in southern Lake Michigan. Wind speed over Lake Michigan was biased low in the NARR atmospheric forcing relative to interpolated wind speed, especially at low wind speed values (Fig. 2), which resulted in important differences in vertical mixing between the two forcing scenarios. Both the interpolated forcing and NARR forcing assimilated wind observations from the northern and southern Lake Michigan buoys, so it was not possible to make an independent comparison to the buoy observations. It is possible that bias was introduced into NARR over-water meteorology through data assimilation, due to the much greater density of surface observations over land than over water.

### *Simulation of surface temperature and thermal stratification*

Simulated thermal structure differed between the two versions of atmospheric forcing. NARR forcing produced greater seasonal variation in surface temperature owing to less surface wind stress. Surface temperature with NARR forcing was colder in February–March and warmer in summer than for interpolated forcing (Fig. 3). Both forcing scenarios simulated surface temperature with reasonable skill although interpolated forcing achieved better skill statistics (Table 1). In comparison to the thermistor chain at the southern Lake Michigan buoy, both forcing scenarios qualitatively reproduced the development of summer stratification, but simulated mixed layer depth was shallower, and thermocline temperature gradient was weaker than observed (Fig. 4).

To objectively quantify SML depth and thermocline gradient, modeled and observed CTD temperature profiles were approximated (least-squares fit) with a 3-layer structure having uniform temperature in the epilimnion and hypolimnion, and a linear temperature gradient in the metalimnion (e.g., Beletsky et al., 2006). SML depth was underpredicted in both forcing scenarios (Table 2, Fig. 5) which was also reported by Beletsky et al. (2006) in POM model simulations. The occurrence of stratified temperature profiles at the locations of the CTD casts was more accurately predicted using interpolated forcing than NARR. Out of 122 total CTD profiles, 32 were observed to be stratified; NARR and interpolated forcing produced 47 and 30 stratified profiles, respectively. Both forcing scenarios underpredicted thermocline gradient (Table 2, Fig. 5). Underprediction of surface mixed layer depth and thermocline temperature gradient has been a persistent problem in three-dimensional numerical models (Beletsky et al., 2006).

The spatial extent and duration of stratification has an important influence on the supply of phytoplankton to benthic filter feeders (Wiles et al., 2006). To quantify the spatial extent and duration of stratification, we used a threshold of $\varphi > 0.4$ J m$^{-3}$ to define the occurrence of stratification, a value that we found produced vertical gradients in chlorophyll concentration in phytoplankton model simulations. The most pronounced difference among the two atmospheric forcing scenarios was increased occurrence of winter stratification in southern Lake Michigan for NARR forcing (Fig. 6).

### *Simulation of currents*

During the unstratified period, current speed and velocity vectors were simulated reasonably well by both forcing scenarios (Table 3, Fig. 7), although NARR forcing produced a notable low bias in current speed. The Fourier norm, $F_n$, values in this study of 0.62–0.72 compare well to other simulations of Lake Michigan currents in winter; Beletsky and Schwab (2001) obtained values of 0.5–0.9 using a 5-km grid POM simulation, while Beletsky et al. (2003) reported values of 0.5–0.71 using a 2-km grid POM simulation with interpolated winds, and improved values of 0.39–0.60 with wind from the MM5 meteorological model. The average angle difference, $\langle\theta\rangle$, values in Table 3 are comparable to values of 0.23–0.46 from a relatively simple 5-km grid barotropic model (Schwab, 1983); $\langle\theta\rangle$ values were not reported in more recent Lake Michigan simulations. As an indicator of the strength of vertical mixing in the unstratified period, we looked at the vertical gradient in current speed (Fig. 7). The vertical gradient was taken from the slope of a linear regression of current speed versus depth for both simulated and observed (ADCP) currents, over the

Please cite this article as: Rowe, M.D., et al., Modeling the effect of invasive quagga mussels on the spring phytoplankton bloom in Lake Michigan, J. Great Lakes Res. (2015), http://dx.doi.org/10.1016/j.jglr.2014.12.018

ARTICLE IN PRESS



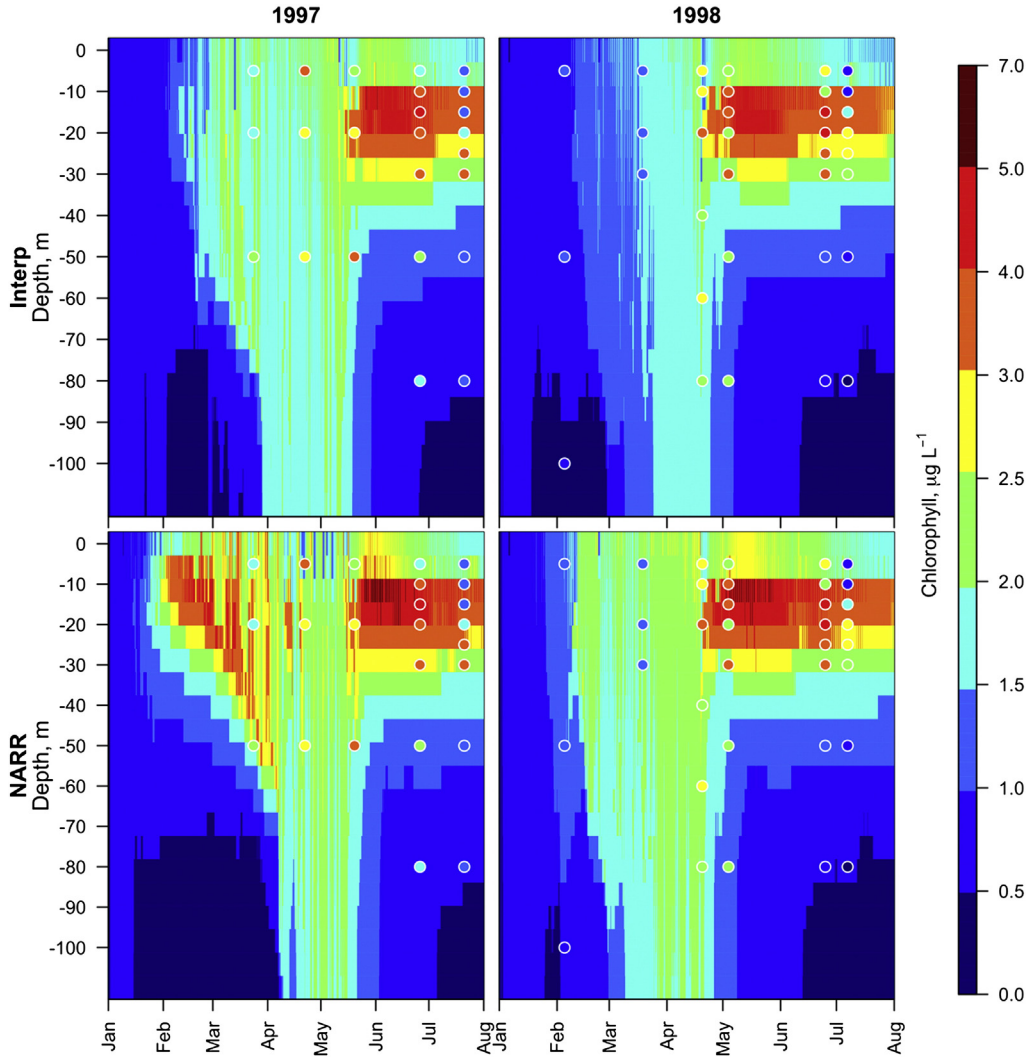


**Fig. 10.** Simulated and observed chlorophyll concentration at the M110 station for 1997 and 1998 under interpolated and NARR forcings. Observed values are given as symbols using the same color bar scale as for the simulated values.

depth range of the observed currents. Both forcing scenarios overestimated the vertical gradient in current speed, as observed by Beletsky et al. (2003) in POM simulations.

Currents during the stratified period were dominated by oscillating currents at a near-inertial period (18 h at the latitude of the ADCP stations), a phenomenon that has been described by others (Beletsky et al., 2006) and is caused by internal Poincaré waves supported by the stratified water column (Troy et al., 2012). Simulation of bottom currents is specifically of interest due to their role in particle resuspension, formation of the benthic nepheloid layer (Hawley, 2004), and potential transport of food particles to benthic filter feeders. Both atmospheric forcing scenarios simulated currents during the stratified period reasonably well (Fig. 8). NARR forcing produced oscillating currents at only the near-inertial period, while interpolated forcing simulated secondary peaks that were observed in the frequency power spectrum (Fig. 9). Model skill statistics were not as good during the stratified period, $0.78 < F_n > 0.99$ (Table 3) as for the unstratified period; small phase shifts in the oscillating currents (e.g. Fig. 8) cause a large penalty in the $F_n$ statistic. The Euler forward time integration scheme, as used in the FVCOM internal mode (Chen et al., 2003), has been shown to produce phase shifts in inertial oscillating currents (Wang and Ikeda, 1997). Bottom current speed was biased low in both forcing scenarios, with greater bias for NARR forcing (Fig. 8, Table 3).

*Phytoplankton model skill assessment*

The interpolated meteorological forcing was selected for phytoplankton model calibration because it had superior skill in simulating the spatial distribution and extent of stratification, relative to NARR forcing. The phytoplankton model was calibrated to produce chlorophyll concentrations that were within the range of observations at station M110 for 1998. Subsequent simulations for 1997 and at other stations used the same set of parameter values. Details of the phytoplankton model calibration are given in ESM along with figures comparing photosynthetic rate, light saturation parameter, growth rate, zooplankton specific ingestion rate, and chlorophyll to carbon ratio to observed values.

The phytoplankton model with interpolated forcing exhibited several features that were consistent with observed seasonal and vertical distribution of chlorophyll (Figs. 10–11) at the M110 station during the spring isothermal and early summer stratified periods. Chlorophyll concentration gradually increased from January until the onset of summer stratification in April or May, and showed little vertical gradient over the depth range of the observations. At the onset of summer stratification, a pronounced chlorophyll maximum formed in the metalimnion and gradually decreased into June and July. Chlorophyll in spring and early summer was also simulated with reasonable skill at the M45 station in 1998 (observations not available in 1997),

Please cite this article as: Rowe, M.D., et al., Modeling the effect of invasive quagga mussels on the spring phytoplankton bloom in Lake Michigan, J. Great Lakes Res. (2015), http://dx.doi.org/10.1016/j.jglr.2014.12.018

ARTICLE IN PRESS



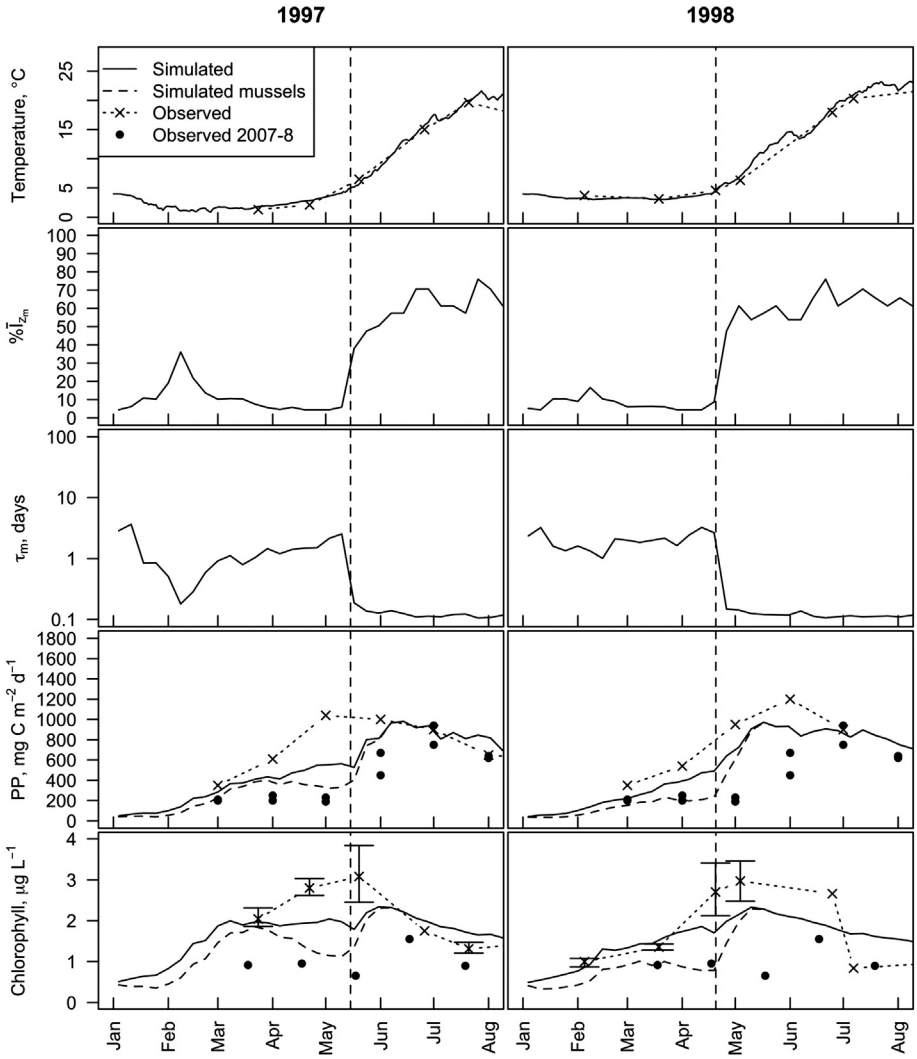


**Fig. 11.** Simulated (lines) and observed (symbols) variables at the M110 station for 1997 and 1998. Temperature, mean irradiance, mixing time scale, and chlorophyll concentration were averaged over the surface mixed layer, while primary production was integrated over the water column. Dashed lines in the lower two panels show simulated chlorophyll and primary production with mussel grazing, and 2007–2008 post-quagga mussel observations (solid circles) are shown for comparison.

although observed chlorophyll declined more rapidly than simulated after the onset of summer stratification (Fig. 14). These results support our assumption that the main features of the spring bloom can be simulated primarily as a function of light and vertical mixing, independent of spatiotemporal variation in nutrient limitation. We used observed values of light-saturated photosynthetic rate for Lake Michigan, which reflected mean nutrient limitation, but spatiotemporal variation in nutrient limitation was not simulated. Simulated SML chlorophyll concentration was higher than observed during midsummer stratification, which likely points to increased importance of nutrient limitation to explain chlorophyll distribution in this time period (Figs. 10–11). In late summer, the observed DCL was deeper and more pronounced than simulated.

The importance of the variable chlorophyll to carbon ratio, $\theta$, parameterization was illustrated by performing a sensitivity trial with $\theta$ fixed at a mean value of 0.038. The simulation with fixed $\theta$ resulted in simulated chlorophyll concentration that was lower than observed during the spring isothermal period and higher than observed in the early summer stratified period (Fig. 12). With variable $\theta$, there was a smaller difference in growth rates between spring isothermal and early stratified periods, which was more consistent with reported growth rates (Fig. S3). In addition, a DCL did not form in simulations with fixed $\theta$. Deepening of the SML in October through December caused an observed increase in SML chlorophyll concentration in both years, which was simulated with variable $\theta$, but not with fixed $\theta$; entrainment of nutrients into the SML from below (not simulated) may be a contributing mechanism to the observed fall increase in chlorophyll, but it is interesting to note that photoacclimation of phytoplankton to decreasing incident irradiance and increasing SML depth may contribute to this phenomenon in addition to nutrient-driven effects.

The influence of vertical mixing on light limitation, and on photoacclimation, were largely responsible for the features of the spring bloom that were accurately simulated. Prior to the onset of summer stratification, deep mixing resulted in low SML mean irradiance; $\%\,\bar{I}_{zm}$ ~5% at the M110 station, consistent with observations by Fahnenstiel et al. (2000). Minor variation in winter stratification (surface < 4 °C) can double $\%\,\bar{I}_{zm}$ to ~10% (Fig. 11) and thereby stimulate phytoplankton growth. Colder surface temperature in March 1997 than in March 1998 resulted in stronger simulated and observed spring bloom in 1997 (Figs. 10, 11). High-biased winter stratification in March 1997 with NARR forcing resulted in high-biased chlorophyll (Fig. 10, lower left panel) for that forcing scenario. Five examples of simulated and observed temperature profiles at M110 are shown in Fig. 13. Stability of the water column, as expressed by potential energy anomaly, was

Please cite this article as: Rowe, M.D., et al., Modeling the effect of invasive quagga mussels on the spring phytoplankton bloom in Lake Michigan, J. Great Lakes Res. (2015), http://dx.doi.org/10.1016/j.jglr.2014.12.018

ARTICLE IN PRESS



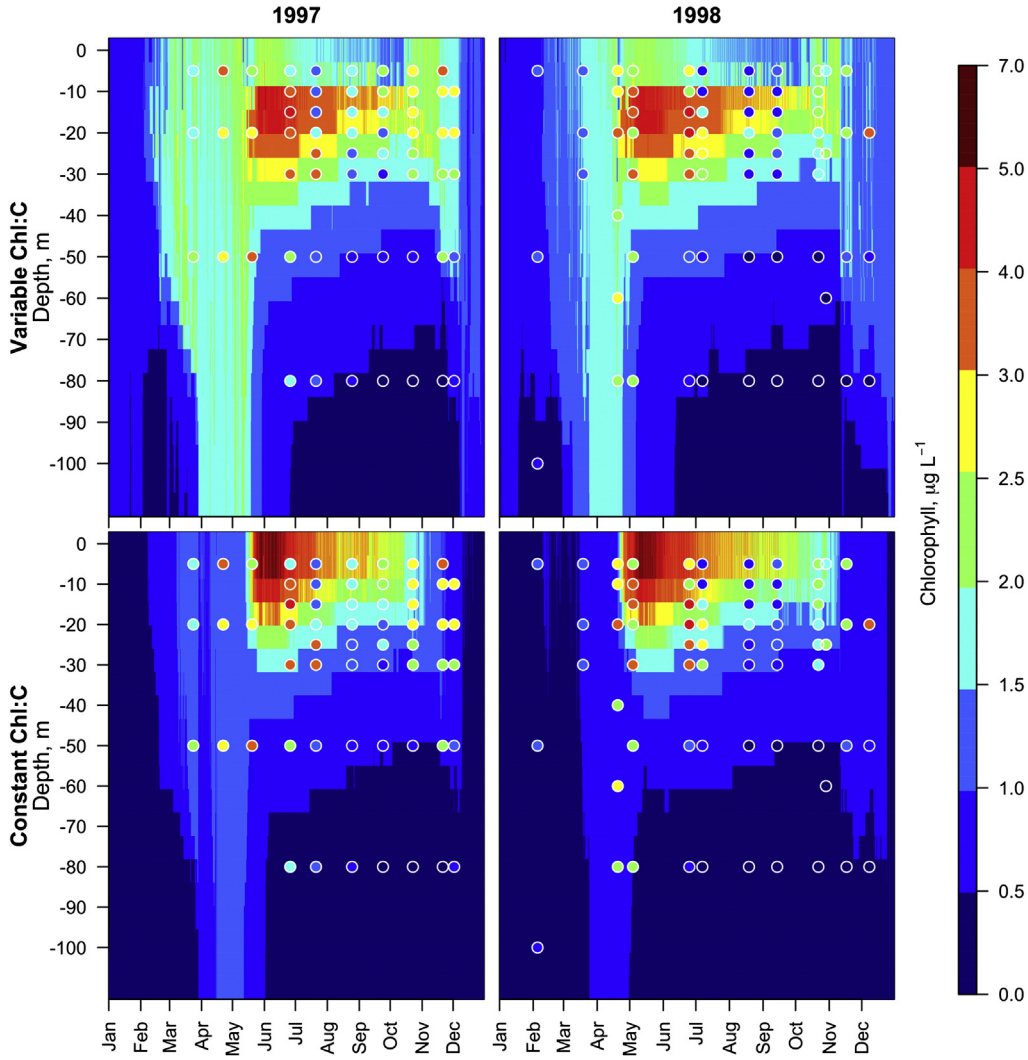


**Fig. 12.** Simulated chlorophyll concentration at the M110 station. Results for the calibrated model are shown in the top panels (with variable Chl:C ratio). Results of a sensitivity trial with Chl:C ratio fixed at a mean value of 0.038 are shown in the bottom panels. Observed values are given as symbols using the same color bar scale as for the simulated values.

accurately simulated with interpolated atmospheric forcing in four of the five cases, while stability with NARR was more often biased high. Both atmospheric forcing scenarios underpredicted stability in April 1997, which caused underprediction of peak chlorophyll in the 1997 spring bloom in both scenarios (Figs. 10–11).

A subsurface maximum occurred in simulated and observed chlorophyll concentrations during summer stratification. Little vertical gradient in chlorophyll concentration occurred prior to summer stratification; the mixing time scale of the SML prior to summer stratification at M110 was ~1 day (Fig. 11), which was much less than the spring

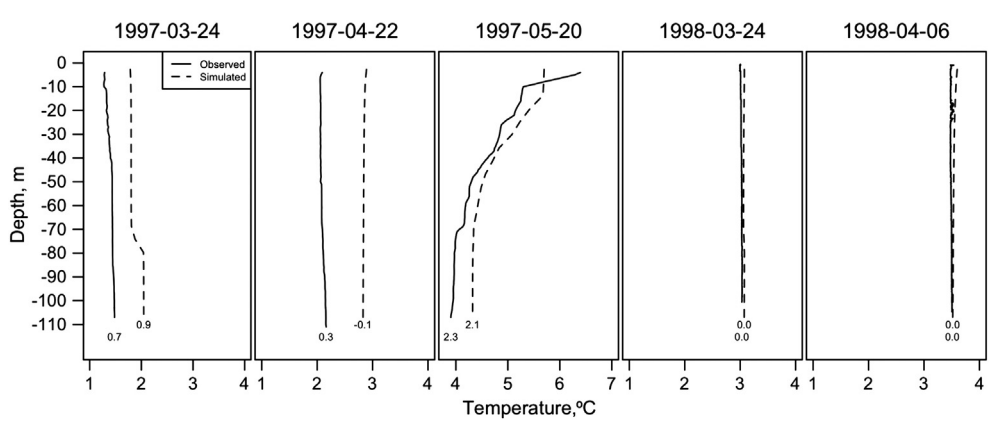


**Fig. 13.** Simulated (interpolated forcing) and observed temperature profiles at the M110 stations on specific dates in March through May of 1997 and 1998. The static stability of the water column is indicated by the potential energy anomaly (J m$^{-3}$), shown as the number below each profile.

Please cite this article as: Rowe, M.D., et al., Modeling the effect of invasive quagga mussels on the spring phytoplankton bloom in Lake Michigan, J. Great Lakes Res. (2015), http://dx.doi.org/10.1016/j.jglr.2014.12.018

ARTICLE IN PRESS



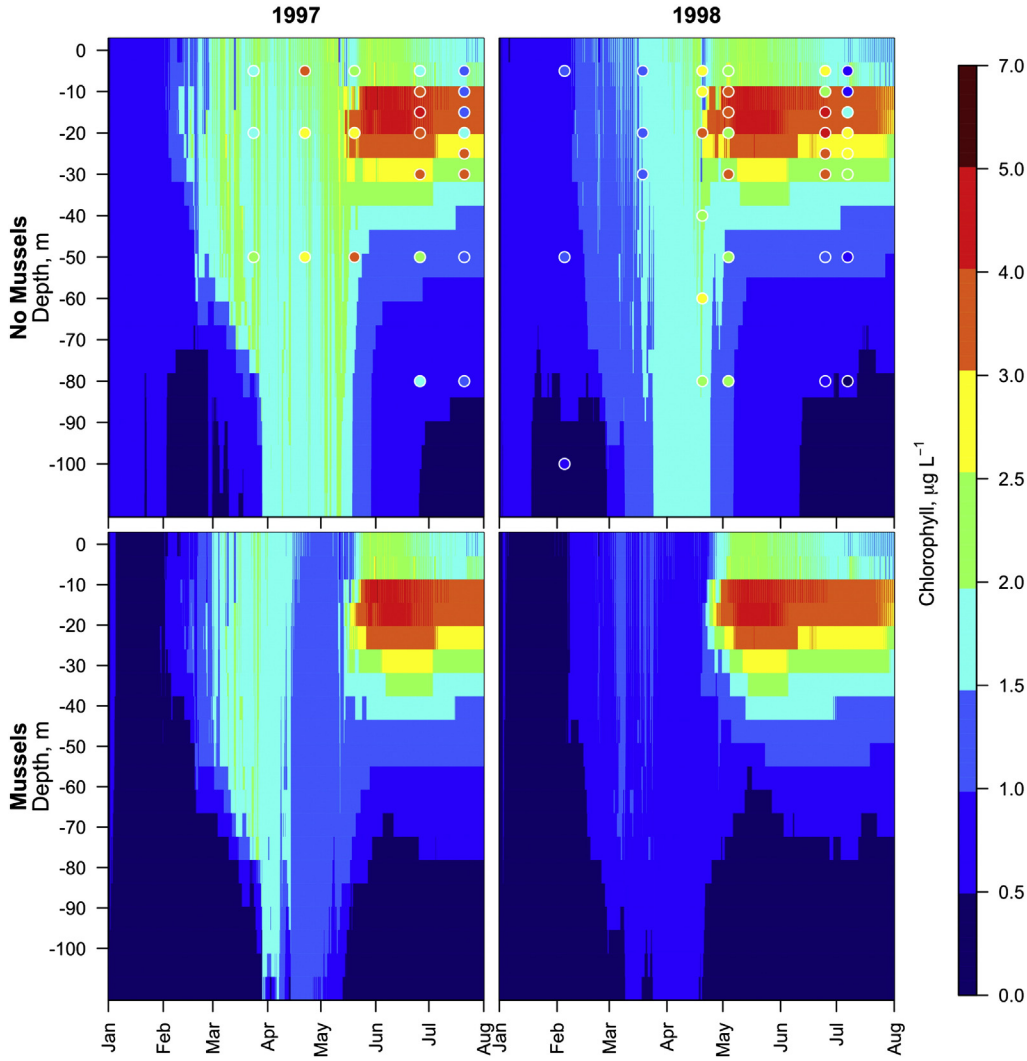


**Fig. 14.** Simulated chlorophyll concentration with and without simulated quagga mussel grazing (M110 station, 1997 and 1998, interpolated forcing). Observed chlorophyll values are shown for the no-mussel scenario.

bloom phytoplankton doubling time of ~11 days (Fahnenstiel et al., 2010). At the onset of summer stratification, % $\bar{I}_{zm}$ increased tenfold to ~60%, greatly stimulating phytoplankton growth. Photoacclimation caused a reduction in SML chl:C ratio, while phytoplankton below the SML in the metalimnion remained shade adapted, resulting in formation of the simulated DCL. Fahnenstiel and Scavia (1987) attributed formation of the DCL in Lake Michigan to a combination of in-situ growth, settling, photoacclimation, and zooplankton grazing. Models that apply a fixed chl:C ratio can produce a DCL (e.g., Bocaniov et al., 2014) by mechanisms other than photoacclimation. For example, a simulated DCL can result from in-situ phytoplankton growth caused by light penetration into a vertical gradient in nutrient concentration in the stratified metalimnion (available phosphorus increasing with depth). Because several mechanisms contribute to formation of the DCL, models will likely vary in their ability to reproduce this phenomenon under different circumstances depending on the mechanisms that are represented.

*Simulated impact of quagga mussel grazing on spring chlorophyll*

To test the hypothesis that the observed decrease in spring chlorophyll and primary production at the M110 station in 2007–8, relative to the 1990s, could be attributed to the direct, local effects of quagga mussel grazing, we applied quagga mussel grazing to phytoplankton simulations at the M110, M45, and M15 stations. Quagga mussel grazing reduced spring chlorophyll and primary production at M110, but did not fully account for the reduction observed in 2007–8 (Figs. 11, 14) relative to 1997–98. The simulated impact of quagga mussel grazing was likely a high-end estimate for several reasons: 1) we applied a mussel biomass of 20 g m$^{-2}$, while observed values at 100-m depth were typically <5 g m$^{-2}$ (Nalepa et al., 2010), 2) we applied a high mussel clearance rate representing a favorable food source, 3) simulated water column stability was biased low in April, 1997 when the greatest simulated mussel impact occurred, and 4) any sub-grid scale benthic boundary layer transport limitation that may exist would further reduce the mussel impact. Therefore, it is unlikely that the observed reduction in chlorophyll and primary production at deep locations such as M110 were caused by direct, local effects of mussel grazing. Mechanisms that were not represented in this model, such as advection of non-local effects of mussel grazing from shallower areas, or mussel-mediated reductions in water column total phosphorus may have contributed to the observed decrease in spring chlorophyll between 1997–98 and 2007–8.

At the shallower M45 station, spring chlorophyll was virtually eliminated by simulated mussel grazing (Fig. 15), but impacts were minimal

Please cite this article as: Rowe, M.D., et al., Modeling the effect of invasive quagga mussels on the spring phytoplankton bloom in Lake Michigan, J. Great Lakes Res. (2015), http://dx.doi.org/10.1016/j.jglr.2014.12.018

ARTICLE IN PRESS



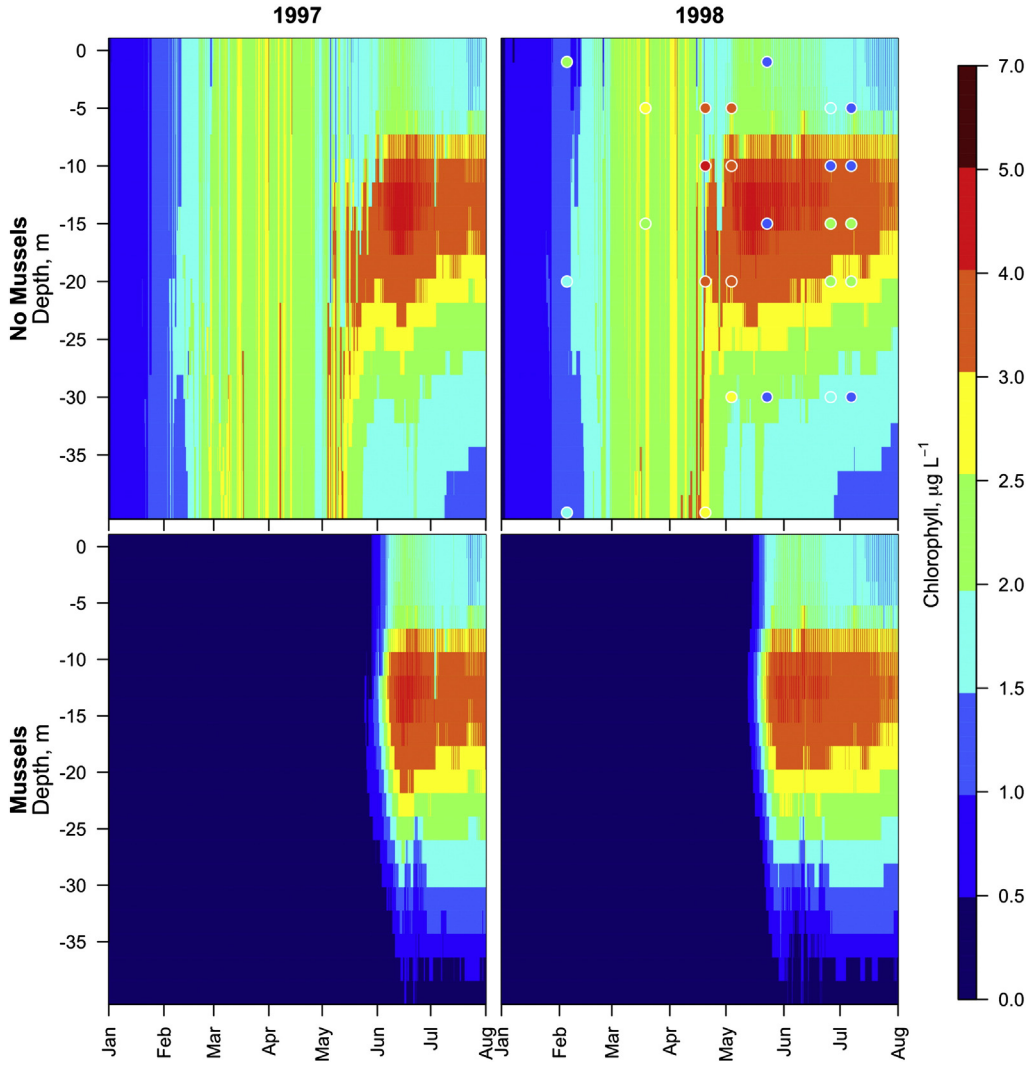


**Fig. 15.** Simulated chlorophyll concentration with and without simulated quagga mussel grazing (M45 station, 1997 and 1998, interpolated forcing). Observed chlorophyll values are shown for the no-mussel scenario in 1998 (observations were not available for 1997).

after onset of summer stratification. At the M15 station, chlorophyll was strongly reduced by mussel grazing in both spring and summer (Fig. 16). At M15, the SML periodically reached the bottom, even during the summer, which provided intermittent transport of phytoplankton to the benthic filter feeders. Our simulation of mussel grazing impact at M15 is a high-end estimate because we applied mussel biomass of 20 g $m^{-2}$ at M15 to be consistent with the M110 and M45 simulations; however, observed biomass was typically <10 g $m^{-2}$ at depth < 30 m (Nalepa et al., 2010).

Mussel grazing impact at M110 was sensitive to inter-annual variation in surface temperature. Enhanced winter stratification in 1997, relative to 1998, stimulated the spring bloom and imposed greater transport limitation on mussel grazing at M110, resulting in greater March and April chlorophyll in 1997 mussel grazing simulations, relative to 1998. However, at M45 and M15, simulated spring chlorophyll was virtually eliminated in mussel grazing scenarios for both 1997 and 1998. While the simulated direct impact of dreissenid filter feeding was less at the 110-m station than at the 45 and 15-m stations, the spring bloom in March and April is concentrated within the 30 to 90-m depth range (Kerfoot et al., 2010; Yousef et al., 2014), In addition, dreissenid mussel biomass is at a maximum within the 30 to 50-m depth range (Nalepa et al., 2009), therefore impacts within the mid-depth (30 to 50-m) range are of particular significance to the spring bloom.

May and June DCL chlorophyll at M110 and M45 were relatively unaffected by simulated mussel grazing. Pothoven and Fahnenstiel (2013) argued that reduced post-mussel DCL chlorophyll in the summer stratified period when lack of vertical mixing cuts off benthic filter feeders from phytoplankton in the metalimnion and epilimnion was caused either by reduced seed stock from the spring bloom to initiate the DCL or by reduced total phosphorus. Our results are more consistent with the latter explanation; even when spring chlorophyll was greatly reduced, simulated DCL formation was relatively unaffected in the absence of altered nutrient limitation. Spring total phosphorus concentration has declined in Lake Michigan since the 1990s, while the ratio of dissolved to particulate phosphorus has increased (Barbiero et al., 2012; Mida et al., 2010). Total phosphorus loads to southern Lake Michigan declined significantly since the 1980s at a rate of about $-1.5\%\ yr^{-1}$, $p = 0.003$ (Mida et al., 2010), while lakewide total phosphorus loads declined at a marginally significant rate of about $-0.7\%\ yr^{-1}$, $p = 0.154$ (Dolan and Chapra, 2012). Declines in phosphorus loading may be partially responsible for the decline in total phosphorus in the water column; however, the observed changes in Lake Michigan since the dreissenid invasion, including reduced phytoplankton chlorophyll, reduced total and particulate phosphorus, increased transparency (Barbiero et al., 2012; Mida et al., 2010), and increased periphyton biomass (Brooks et al., 2014), are consistent with changes that have been observed in lakes invaded by dreissenid mussels across North America and Europe

Please cite this article as: Rowe, M.D., et al., Modeling the effect of invasive quagga mussels on the spring phytoplankton bloom in Lake Michigan, J. Great Lakes Res. (2015), http://dx.doi.org/10.1016/j.jglr.2014.12.018

ARTICLE IN PRESS



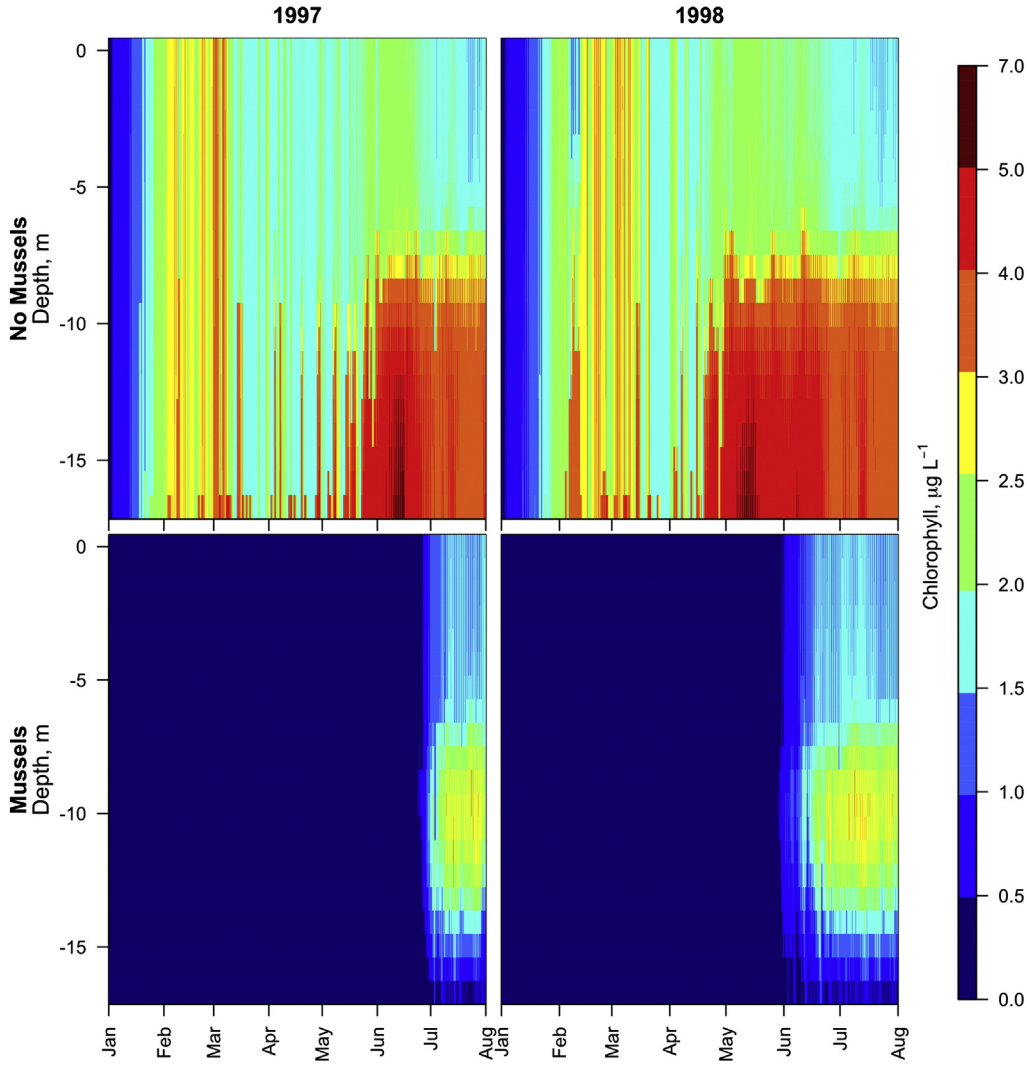


**Fig. 16.** Simulated chlorophyll concentration with and without simulated quagga mussel grazing (M15 station, 1997 and 1998, interpolated forcing). Observed chlorophyll was not available at M15.

(Higgins, 2014). Our model simulations show that the direct effects of dreissenid filter feeding can account for disappearance of the spring bloom when the water column is vertically well-mixed, with strong reductions in phytoplankton abundance at intermediate depths of ~45 m where dreissenid biomass is highest, and where the spring bloom was historically concentrated. However, stratification isolates the euphotic zone from profundal dreissenid filter feeding for the majority of the year, including periods of winter stratification (e.g., Fig. 6), and direct, local effects of dreissenid filter feeding cannot account for observed reductions in phytoplankton abundance in stratified periods, suggesting a partial contribution of reduced total phosphorus concentrations.

## Conclusions

A 3D hydrodynamic simulation of Lake Michigan, 1998, using FVCOM exhibited similar overall skill in simulating temperature profiles and currents to prior simulations reported in the literature using POM. Interpolated atmospheric forcing, as used in the NOAA Great Lakes Coastal Forecasting System, resulted in greater skill in simulation of physical variables of importance to the lower food web than NARR atmospheric forcing and should be used for studies of the Great Lakes when available in place of NARR. Atmospheric forcing from NARR had lower over-lake wind speeds than interpolated forcing, which resulted in reduced current speeds, increased summer surface temperature, and increased spatial extent and duration of stratification in winter and summer.

A 1-D column phytoplankton model simulated seasonal and vertical distribution of chlorophyll in January through June with reasonable skill, without simulating spatiotemporal variation in nutrient limitation, highlighting the importance of vertical mixing, light limitation, and photoacclimation as controlling mechanisms during this time period. Simulated surface chlorophyll during July to October was biased high, suggesting that the influence of nutrient limitation on chlorophyll distribution is of greater importance during this period than in January through June. Simulations that included the variable chl:C ratio photoacclimation model of Geider et al. (1997) better approximated the seasonal and vertical distribution of chlorophyll concentration than simulations with fixed chl:C ratio. The phytoplankton model successfully simulated greater chlorophyll concentrations at the M110 (110-m depth) station in March and April of 1997, relative to 1998, suggesting that the difference was caused by reduced light limitation as a result of enhanced winter stratification by colder conditions in 1997.

Phytoplankton simulations with mussel filter feeding at stations of 110, 45, and 15-m depth produced strong reductions in chlorophyll at times when the water column was mixed to the bottom. Simulated mussel filter feeding had little effect on chlorophyll during periods of summer and winter stratification. These model simulations did not

Please cite this article as: Rowe, M.D., et al., Modeling the effect of invasive quagga mussels on the spring phytoplankton bloom in Lake Michigan, J. Great Lakes Res. (2015), http://dx.doi.org/10.1016/j.jglr.2014.12.018

account for possible effects of quagga mussels on phosphorus cycling, or advection of non-local grazing impacts in shallower areas; these mechanisms could contribute to reductions in chlorophyll during stratified periods, which has been reported in the literature. These model simulations highlight the sensitivity of both phytoplankton growth and the impact of profundal quagga mussel filter feeding to vertical mixing and stratification, which in turn is controlled by meteorological conditions.

## Acknowledgments

M.D. Rowe received funding through the National Research Council Research Associate program. The authors gratefully acknowledge Steven Pothoven, NOAA GLERL Lake Michigan Field Station, for providing chlorophyll concentration measurements. This is GLERL Contribtion No. 1743.

## Appendix A. Supplementary data

Supplementary data to this article can be found online at http://dx.doi.org/10.1016/j.jglr.2014.12.018.

## References

Bai, X., Wang, J., Schwab, D.J., Yang, Y., Luo, L., Leshkevich, G.A., Liu, S., 2013. Modeling 1993–2008 climatology of seasonal general circulation and thermal structure in the Great Lakes using FVCOM. Ocean Model. 65, 40–63.

Barbiero, R., Lesht, B., Warren, G., 2012. Convergence of trophic state and the lower food web in Lakes Huron, Michigan and Superior. J. Great Lakes Res. 38 (2), 368–380.

Beletsky, D., Schwab, D., 2001. Modeling circulation and thermal structure in Lake Michigan: annual cycle and interannual variability. J. Geophys. Res. 106 (C9), 19745–19771.

Beletsky, D., Schwab, D., Roebber, P., McCormick, M., Miller, G., Saylor, J., 2003. Modeling wind-driven circulation during the March 1998 sediment resuspension event in Lake Michigan. J. Geophys. Res. Oceans 108 (C2), 3038. http://dx.doi.org/10.1029/2001JC001159.

Beletsky, D., Schwab, D., McCormick, M., 2006. Modeling the 1998–2003 summer circulation and thermal structure in Lake Michigan. J. Geophys. Res. Oceans 111 (C10), 1–18.

Bleiker, W., Schanz, F., 1997. Light climate as the key factor controlling the spring dynamics of phytoplankton in Lake Zürich. Aquat. Sci. Res. Across Boundaries 59 (2), 135–157.

Bocaniov, S.A., Smith, R.E., Spillman, C.M., Hipsey, M.R., Leon, L.F., 2014. The nearshore shunt and the decline of the phytoplankton spring bloom in the Laurentian Great Lakes: insights from a three-dimensional lake model. Hydrobiologia 731 (1), 151–172.

Brooks, C., Grimm, A., Shuchman, R., Sayers, M., Jessee, N., 2014. A satellite-based multi-temporal assessment of the extent of nuisance *Cladophora* and related submerged aquatic vegetation for the Laurentian Great Lakes. Remote Sens. Environ. http://dx.doi.org/10.1016/j.rse.2014.04.032.

Cerco, C.F., Noel, M.R., 2004. Process-based primary production modeling in Chesapeake Bay. Mar. Ecol. Prog. Ser. 282, 45–58.

Chen, C., Liu, H., Beardsley, R.C., 2003. An unstructured grid, finite-volume, three-dimensional, primitive equations ocean model: application to coastal ocean and estuaries. J. Atmos. Ocean. Technol. 20 (1), 159–186.

Chen, C.S., Wang, L.X., Ji, R.B., Budd, J.W., Schwab, D.J., Beletsky, D., Fahnenstiel, G.L., Vanderploeg, H., Eadie, B., Cotner, J., 2004. Impacts of suspended sediment on the ecosystem in Lake Michigan: a comparison between the 1998 and 1999 plume events. J. Geophys. Res. Oceans 109 (C10). http://dx.doi.org/10.1029/2002JC001687.

Croley, T.E., 1989. Verifiable evaporation modeling on the Laurentian Great Lakes. Water Resour. Res. 25 (5), 781–792.

Dolan, D., Chapra, S., 2012. Great Lakes total phosphorus revisited: 1. Loading analysis and update (1994–2008). J. Great Lakes Res. 38 (4), 730–740.

Fahnenstiel, G., Scavia, D., 1987. Dynamics of Lake Michigan phytoplankton: the deep chlorophyll layer. J. Great Lakes Res. 13 (3), 285–295.

Fahnenstiel, G.L., Chandler, J.F., Carrick, H.J., Scavia, D., 1989. Photosynthetic characteristics of phytoplankton communities in Lakes Huron and Michigan: PI parameters and end-products. J. Great Lakes Res. 15 (3), 394–407.

Fahnenstiel, G.L., Krause, A.E., McCormick, M.J., Carrick, H.J., Schelske, C.L., 1998. The structure of the planktonic food-web in the St. Lawrence Great Lakes. J. Great Lakes Res. 24 (3), 531–554.

Fahnenstiel, G.L., Stone, R.A., McCormick, M.J., Schelske, C.L., Lohrenz, S.E., 2000. Spring isothermal mixing in the Great Lakes: evidence of nutrient limitation and nutrient–light interactions in a suboptimal light environment. Can. J. Fish. Aquat. Sci. 57 (9), 1901–1910.

Fahnenstiel, G.L., Pothoven, S., Vanderploeg, H., Klarer, D., Nalepa, T., Scavia, D., 2010. Recent changes in primary production and phytoplankton in the offshore region of southeastern Lake Michigan. J. Great Lakes Res. 36, 20–29.

Fairall, C., Bradley, E., Rogers, D., Edson, J., Young, G., 1996. Bulk parameterization of air–sea fluxes for tropical ocean–global atmosphere coupled–ocean atmosphere response experiment. J. Geophys. Res. 101 (C2), 3747–3764.

Fulton, E.A., Smith, A.D.M., Johnson, C.R., 2003. Mortality and predation in ecosystem models: is it important how these are expressed? Ecol. Model. 169 (1), 157–178.

Galperin, B., Kantha, L., Hassid, S., Rosati, A., 1988. A quasi-equilibrium turbulent energy model for geophysical flows. J. Atmos. Sci. 45 (1), 55–62.

Geider, R.J., Osborne, B.A., 1989. Respiration and microalgal growth: a review of the quantitative relationship between dark respiration and growth. New Phytol. 112 (3), 327–341.

Geider, R., MacIntyre, H., Kana, T., 1997. Dynamic model of phytoplankton growth and acclimation: responses of the balanced growth rate and the chlorophyll a:carbon ratio to light, nutrient-limitation and temperature. Mar. Ecol. Prog. Ser. 148 (1), 187–200.

Geider, R.J., MacIntyre, H.L., Kana, T.M., 1998. A dynamic regulatory model of phytoplanktonic acclimation to light, nutrients, and temperature. Limnol. Oceanogr. 43 (4), 679–694.

Hawley, N., 2004. Response of the benthic nepheloid layer to near-inertial internal waves in southern Lake Michigan. J. Geophys. Res. Oceans 109 (C4), 1–14.

Higgins, S.N., 2014. Meta-analysis of dreissenid effects on freshwater ecosystems. In: Nalepa, T.F., Schloesser, D.W. (Eds.), Quagga and Zebra Mussels: Biology, Impacts and Control, 2nd ed. CRC Press, Boca Raton, FL, pp. 487–494.

Kerfoot, W.C., Yousef, F., Green, S.A., Budd, J.W., Schwab, D.J., Vanderploeg, H.A., 2010. Approaching storm: disappearing winter bloom in Lake Michigan. J. Great Lakes Res. 36 (Suppl. 3), 30–41.

Kim, T.J., Khangaonkar, T., 2012. An offline unstructured biogeochemical model (UBM) for complex estuarine and coastal environments. Environ. Model Softw. 31, 47–63.

Lang, G.A., Fahnenstiel, G.L., 1996. Great Lakes primary production model—methodology and use. NOAA Tech. Memo. ERL GLERL-90. NOAA Great Lakes Environ. Lab., Ann Arbor, MI (ftp://ftp.glerl.noaa.gov/publications/tech_reports/glerl-090/tm-090.pdf).

Luo, L., Wang, J., Schwab, D., Vanderploeg, H., Leshkevich, G., Bai, X., Hu, H., Wang, D., 2012. Simulating the 1998 spring bloom in Lake Michigan using a coupled physical–biological model. J. Geophys. Res. Oceans 117, C10011. http://dx.doi.org/10.1029/2012JC008216.

Mesinger, F., DiMego, G., Kalnay, E., Mitchell, K., Shafran, P., Ebisuzaki, W., Jovic, D., Woollen, J., Rogers, E., Berbery, E., 2006. North American regional reanalysis. Bull. Am. Meteorol. Soc. 87 (3), 343–360.

Mida, J.L., Scavia, D., Fahnenstiel, G.L., Pothoven, S.A., Vanderploeg, H.A., Dolan, D.M., 2010. Long-term and recent changes in southern Lake Michigan water quality with implications for present trophic status. J. Great Lakes Res. 36 (sp3), 42–49.

Nalepa, T.F., Fanslow, D.L., Lang, G.A., 2009. Transformation of the offshore benthic community in Lake Michigan: recent shift from the native amphipod *Diporeia* spp. to the invasive mussel *Dreissena rostriformis bugensis*. Freshw. Biol. 54 (3), 466–479.

Nalepa, T.F., Fanslow, D.L., Pothoven, S.A., 2010. Recent changes in density, biomass, recruitment, size structure, and nutritional state of Dreissena populations in southern Lake Michigan. J. Great Lakes Res. 36 (SP3), 5–19.

Parkinson, C., Washington, W., 1979. A large-scale numerical model of sea ice. J. Geophys. Res. Oceans 84 (C1), 311–337.

Pauer, J.J., Anstead, A.M., Melendez, W., Rossmann, R., Taunt, K.W., Kreis, R.G., 2008. The Lake Michigan eutrophication model, LM3-Eutro: model development and calibration. Water Environ. Res. 80 (9), 853–861.

Phillips, W.D., Irbe, J.G., 1978. Land-to-lake comparison of wind, temperature, and humidity on Lake Ontario during the International Field Year for the Great Lakes (IFYGL). Atmospheric Environment Service, Environment Canada, Downsview, ON, p. 51.

Pothoven, S.A., Fahnenstiel, G.L., 2013. Recent change in summer chlorophyll a dynamics in southeastern Lake Michigan. J. Great Lakes Res. 39 (2), 287–294.

Ross, O.N., Geider, R.J., Berdalet, E., Artigas, M.L., Piera, J., 2011. Modelling the effect of vertical mixing on bottle incubations for determining in situ phytoplankton dynamics. I. Growth rates. Mar. Ecol. Prog. Ser. 435, 33–45.

Scavia, D., Lang, G.A., Kitchell, J.F., 1988. Dynamics of Lake Michigan plankton: a model evaluation of nutrient loading, competition, and predation. Can. J. Fish. Aquat. Sci. 45 (1), 165–177.

Schwab, D., 1983. Numerical simulation of low-frequency current fluctuations in Lake Michigan. J. Phys. Oceanogr. 13 (12), 2213–2224.

Schwab, D.J., Beletsky, D., 1998. Lake Michigan Mass Balance Study: Hydrodynamic Modeling Project. ERL GLERL-108. NOAA GLERL, Ann Arbor, MI, p. 53.

Schwab, D., Morton, J., 1984. Estimation of overlake wind speed from overland wind speed: a comparison of three methods. J. Great Lakes Res. 10 (1), 68–72.

Simpson, J., Bowers, D., 1981. Models of stratification and frontal movement in shelf seas. Deep-Sea Res. 28 (7), 727–738.

Troy, C., Ahmed, S., Hawley, N., Goodwell, A., 2012. Cross-shelf thermal variability in southern Lake Michigan during the stratified periods. J. Geophys. Res. 117, C02028. http://dx.doi.org/10.1029/2011JC007148.

Vanderploeg, H.A., Johengen, T.H., Lavrentyev, P.J., Chen, C., Lang, G.A., Agy, M.A., Bundy, M.H., Cavaletto, J.F., Eadie, B.J., Liebig, J.R., Miller, G.S., Ruberg, S.A., McCormick, M.J., 2007. Anatomy of the recurrent coastal sediment plume in Lake Michigan and its impacts on light climate, nutrients, and plankton. J. Geophys. Res. 112, C03S90. http://dx.doi.org/10.1029/2004JC002379.

Vanderploeg, H.A., Liebig, J.R., Nalepa, T.F., Fahnenstiel, G.L., Pothoven, S.A., 2010. *Dreissena* and the disappearance of the spring phytoplankton bloom in Lake Michigan. J. Great Lakes Res. 36 (sp3), 50–59.

Vanderploeg, H., Pothoven, S., Fahnenstiel, G., Cavaletto, J., Liebig, J., Stow, C., Nalepa, T., Madenjian, C., Bunnell, D., 2012. Seasonal zooplankton dynamics in Lake Michigan: disentangling impacts of resource limitation, ecosystem engineering, and predation during a critical ecosystem transition. J. Great Lakes Res. 38 (2), 336–352.

Wang, J., Ikeda, M., 1997. Inertial stability and phase error of time integration schemes in ocean general circulation models. Mon. Weather Rev. 125 (9), 2316–2327.

ARTICLE IN PRESS



Wang, J., Bai, X., Hu, H., Clites, A., Colton, M., Lofgren, B., 2012. Temporal and spatial variability of Great Lakes ice cover, 1973–2010. J. Clim. 25 (4), 1318–1329.
White, B., Austin, J., Matsumoto, K., 2012. A three-dimensional model of Lake Superior with ice and biogeochemistry. J. Great Lakes Res. 38 (1), 61–71.
Wiles, P., van Duren, L., Häse, C., Larsen, J., Simpson, J., 2006. Stratification and mixing in the Limfjorden in relation to mussel culture. J. Mar. Syst. 60 (1), 129–143.
Yousef, F., Charles, Kerfoot W., Shuchman, R., Fahnenstiel, G., 2014. Bio-optical properties and primary production of Lake Michigan: insights from 13-years of SeaWiFS imagery. J. Great Lakes Res. 40 (2), 317–324.
Zhang, H., Culver, D.A., Boegman, L., 2011. Dreissenids in Lake Erie: an algal filter or a fertilizer? Aquat. Invasions 6 (2), 175–194.

Please cite this article as: Rowe, M.D., et al., Modeling the effect of invasive quagga mussels on the spring phytoplankton bloom in Lake Michigan, J. Great Lakes Res. (2015), http://dx.doi.org/10.1016/j.jglr.2014.12.018